Synthesis of L-Lysine-based phosphonate PAMAM 'Janus' dendrimers

Quirijn van Dierendonck, BSc

890928182040

Supervisors

Medea Kosian, MSc

Dr. Ir. Maarten Smulders

Prof. Dr. Han Zuilhof

Laboratory of Organic Chemistry

Wageningen University

29/09/2015

Acknowledgement

I would like to thank my direct supervisors Maarten Smulders and Medea Kosian for all their help in bringing this thesis to its close. Without their understanding of my situation, their patience and their help I don't think I would have been able to finish this project the way I did. I would also like to thank Han Zuilhof, for his support, understanding and the occasional proverbial 'kick' to get me going. A big thanks also go to Pepijn Geutjes, for his help with the NMR techniques, and to Frank Claassen, for his help with the MS.

Finally, I would like to thank everybody at ORC for their support, help and the nice working atmosphere!

Table of Contents

Summary ..... - 4 -
Introduction ..... - 5 -
Stainless steel ..... - 5 -
Surface modification ..... - 5 -
Phosphonic acids ..... - 5 -
Dendrimers ..... - 6 -
Objective ..... - 7 -
Experimental design ..... - 8 -
Synthetic route ..... - 8 -
Results and Discussion ..... - 10 -
Amide coupling ..... - 10 -
Aza-Michael addition ..... - 12 -
Bi-adduct – Generation 1 dendron ..... - 12 -
Tetra-adduct – Generation 2 dendron ..... - 21 -
Reductive amination ..... - 30 -
Conclusions ..... - 36 -
Future work ..... - 37 -
References ..... - 39 -
Supporting Information ..... - 41 -
Experimental section ..... - 41 -
NMR spectra ..... - 46 -
MS spectra ..... - 54 -

Summary

Stainless steel is an abundant material in modern industry, because of its flexibility in use and its interesting properties, such as resistance against oxidative corrosion and acidic/basic corrosion. Adding desired functionalities or additional protection to stainless steel is a very appealing prospect for many branches of modern industry. Introducing these functionalities can be done in various ways, including self-assembled monolayers or coatings with particles or dendrimers. Dendrimers in particular are a good way to introduce functionalities to stainless steel, because of their ability to form multiple attachments to the surface, thus strengthening the adhesion. This adhesion to stainless steel can be obtained by using dendrimers containing terminal phosphonates, which have been proven to form strong bonds with stainless steel when used in surface chemistry.

During this project, the synthesis of a phosphonic acid modified dendron starting from L-lysine was explored, which would be used to create PAMAM 'Janus' dendrimers that can be grafted to stainless steel SS316L. Multiple pathways were examined, resulting in the suggestion of several different pathways to yield both generation 1 and generation 2 dendrons. Although no actual dendrons could be isolated and characterized, key reactions of the proposed pathways were analysed by MS and NMR, the results of which suggest that the reactions, and thereby the pathways, are viable ways to yield a phosphonate-functionalised L-lysine PAMAM dendron of either generation 1 or generation 2.

Introduction

Stainless steel

Stainless steel is often used in modern industrial processes. This is mostly due to its resistance to corrosion, its strength and relatively easy fabrication. Stainless steel is an alloy chemically composed of iron and carbon, containing a minimum of 10.5% w.t. of chromium. The addition of the chromium prevents the oxidation of the carbon iron steel, which oxidizes readily in moist air, by forming a passive layer [1] of octahedral coordinated Cr(III) ions bearing terminal hydroxyl and water ligands at the interface with air (Figure 1). While the most common grade of stainless steel is type 304, which contains 0.15% carbon, 18% chromium and 8% nickel, for highly corrosive or saline environments type 316 is more suitable due to the inclusion of 2.5% molybdenum. This alloy has a higher corrosion resistance than other types of steel [2, 3].

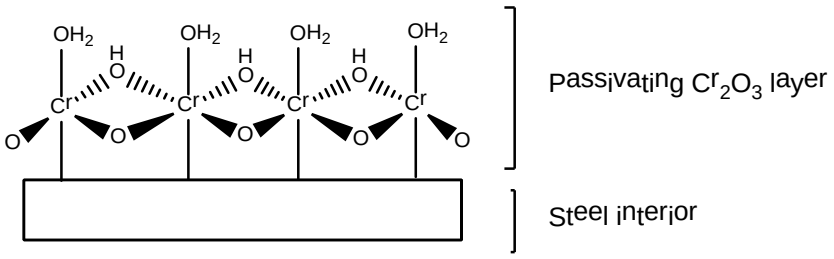

Figure 1. Surface of stainless steel, showing the coordination of the Cr(III) layer

As machinery gets progressively scaled down in size, surface properties and forces on stainless steel start playing larger roles as well as on all other surfaces. However, even the macro scale modification of stainless steel is a desirable goal. Therefore, coating stainless steel surfaces with organic monolayers is becoming increasingly favourable.

Surface modification

Research on the modification of surfaces has flourished over the last decades and has kept shrinking down the scale at which these modifications take place. However, when the scale shrinks down to the nanoscale, surface properties and chemistry become important [4]. By applying self-assembling monolayers (SAMs) of organic monolayer to inorganic surfaces, the properties and chemistry of these surfaces can be countered, changed or enhanced to fine-tune the surface for its intended function.

Phosphonic acids

One group of organic compounds favoured in the formation of monolayers on metal oxide surfaces is comprised of phosphonic acids and their salts and esters. The fact that phosphonic acid containing molecules formed adsorbed films on metal surfaces has been known since 1954 [5], but the fact that phosphonic acids react readily with a wide range of metal salts and oxides via a very stable P-O-M bond was only discovered during the late 1970s [6]. Due to this reactivity towards metal and transition metals containing supports (oxides, hydroxides, carbonates, phosphates e.g.) [7], phosphonate monolayers have been grafted to a wide variety of metal oxide surfaces, including common engineering metals like stainless steel [8], steel, aluminium, copper and brass [9], but also alumina particles [10], indium tin oxide [11] and medically interesting metals like titanium [12], titanium dioxide and zirconium dioxide [13]. Phosphonates can even be grafted to human bone [14, 15].

SAMs of phosphonate containing molecules have already been grafted to different kinds of steel to inhibit corrosion of the metal in aqueous media [16, 17, 18, 19] and have also been used to create

antibacterial coatings on stainless steel [20]. Other applications rising from grafting phosphonate SAMs on metal surfaces include the use in organic field-effect transistors [21], organic thin-film transistors [22], selective patterning techniques for molecular assembly [23] and decreasing the growth of tumour cells, pathogenic protozoa and some bacteria [15]. These diverse applications indicate that phosphonic acid SAMs are a very powerful tool to impart additional or specific functionality to a commonly used material like stainless steel. However, the more phosphonate moieties, the stronger the interaction with the surface. While single molecules can contain more than one phosphonate group, they can become very difficult to synthesise. Therefore, a simple-to-synthesise molecule with multiple phosphonate groups would be ideal to modify the surface of stainless steel.

Dendrimers

Since their discovery [24], the molecules initially known as starburst-dendritic macromolecules have been researched extensively because of their very appealing characteristics, which include the fact that dendrimers are essentially monodisperse single compounds with very defined chemical properties. The original concept of the dendrimer was built on a structure with branches of symmetrical molecules, that when repeated formed a very well-defined structure. This does not mean that all repeats have to be symmetrical, as in the case of L-lysine, where the chirality is very advantageous in the design of poly(amidoamine) or PAMAM dendrimers [25, 26].

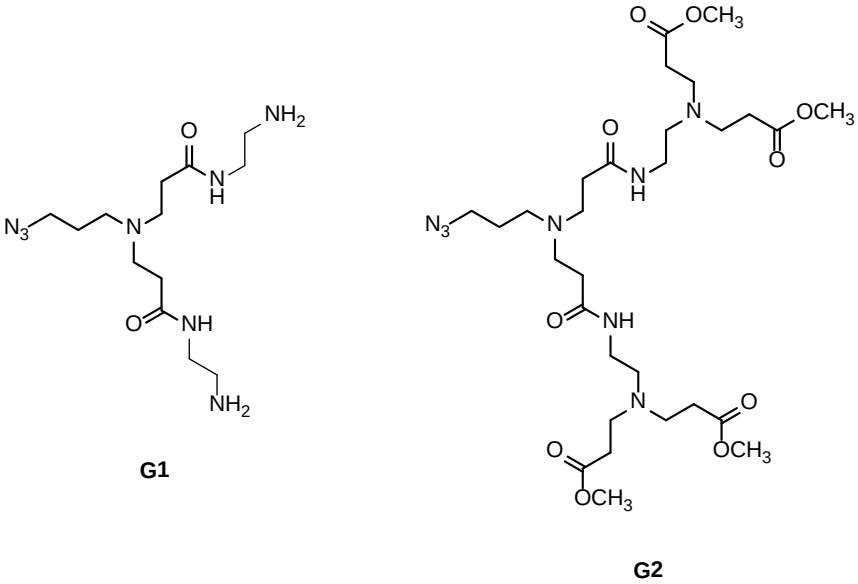

Figure 2. Examples of a PAMAM dendron of 3-azidopropan-1-amine reacted with methyl acrylate, where G1 is a first generation dendron and G2 a second generation dendron

The structure of a dendrimer is composed of three distinct regions: 1) a core, 2) layers of branched repeats attached to the core and 3) specific end groups on the outer layer of the repeat units [27]. As an example, in Figure 2 the core of the dendron is the chain containing the azide, methyl acrylate the repeat and the methyl ester the outer layer with end groups. The chemical nature of the end groups dominate the properties of the dendrimer as the dendrimer increases in size, as the number of end groups increases exponentially with each layer of repeats (also called generation or **G**).

Two synthetic approaches exist at present to synthesise dendrimers: the divergent and the convergent approach. The divergent approach, which arose from the earliest work on dendrimer synthesis [24, 28], grows the dendrimer outwards from the core, adding layer after layer of repeats until the end groups are coupled last. The convergent approach, which was reported about 5 years after the first

classification of dendrimers [29], grows the dendrimer inwards from the end groups, synthesising dendrons that are coupled to the core to finish the dendrimer.

Some dendrimers can be synthesised with the dendrimer containing two hemispheres with different end groups, leading to the dendrimer having different chemical properties on each hemisphere [25]. These dendrimers, often called 'Janus' dendrimers after the ancient two-headed Roman god that watched both the front and rear door at the same time, are obtained by coupling two dendrons with different end groups at their core [30]. This is very useful, as one dendron can be synthesised to contain groups dedicated to providing a strong interaction with the surface, while the second dendron contains groups which can, for instance, be used to give biological activity to the surface.

Objective

There are multiple reasons for choosing L-lysine as the starting point for a dendrimer. First, while L-lysine itself is not a symmetrical molecule, unlike those so often used in the creation of dendrimeric compounds, its inherent chirality creates an asymmetric dendrimer structure when compared to the more common symmetric dendrimers. This will enable comparison studies with symmetric dendrimers based on the symmetric 6-aminocaproic acid, which were earlier created by Medea Kosian. Second, the inclusion of two primary amines and a carboxylic acid group in the molecule gives access to some fairly straightforward reactions to create dendrimers.

The Michael addition is a simple addition reaction, where a nucleophile facilitates an addition to an α,β-unsaturated carbonyl compound [31]. In case of the aza-Michael addition, the nucleophile is nitrogen based. This reaction is an excellent way to introduce branching in the L-lysine dendrimer, as primary amines are able to perform this addition twice.

A way to introduce functionality to the dendrimer, is via amide coupling reactions using carbodiimides, like carbonyldiimidazole (CDI). This can even be done under solvent-free conditions [32, 33], which can make the purification of reactions easier, can speed up the reaction significantly and also make the reaction 'greener' by eliminating the use of organic solvents [34]. In case of the L-lysine-based dendrimer, amide coupling reactions can be used to introduce the phosphonic acid functionality and to introduce a group capable of undergoing 'click' chemistry, like an alkyne group to facilitate an copper-catalysed azido-alkyne Huisgen cycloaddition. This would make the merging of two different dendrons into a finished 'Janus' dendrimer relatively easy.

In this project, the synthesis of a L-lysine PAMAM 'Janus' dendrimer was explored, that would be grafted to stainless steel SS316L surfaces. The focus fell on a L-lysine **G1** dendron containing phosphonic acid groups to facilitate the grafting of the finished dendrimers on the steel surface. Introducing the phosphonic acid groups and 'click' functionality would be achieved by using CDI-mediated amide coupling reactions under solvent-free conditions, while the aza-Michael addition would be used to facilitate the creation of **G2** dendrons or larger.

Experimental design

Synthetic route

To synthesise one of the dendrons of a PAMAM 'Janus' dendrimer, the following route is proposed. The starting material for this project was L-lysine, which through several steps gives the final diphosphonate dendron. The synthesis steps are shown in Scheme 1.

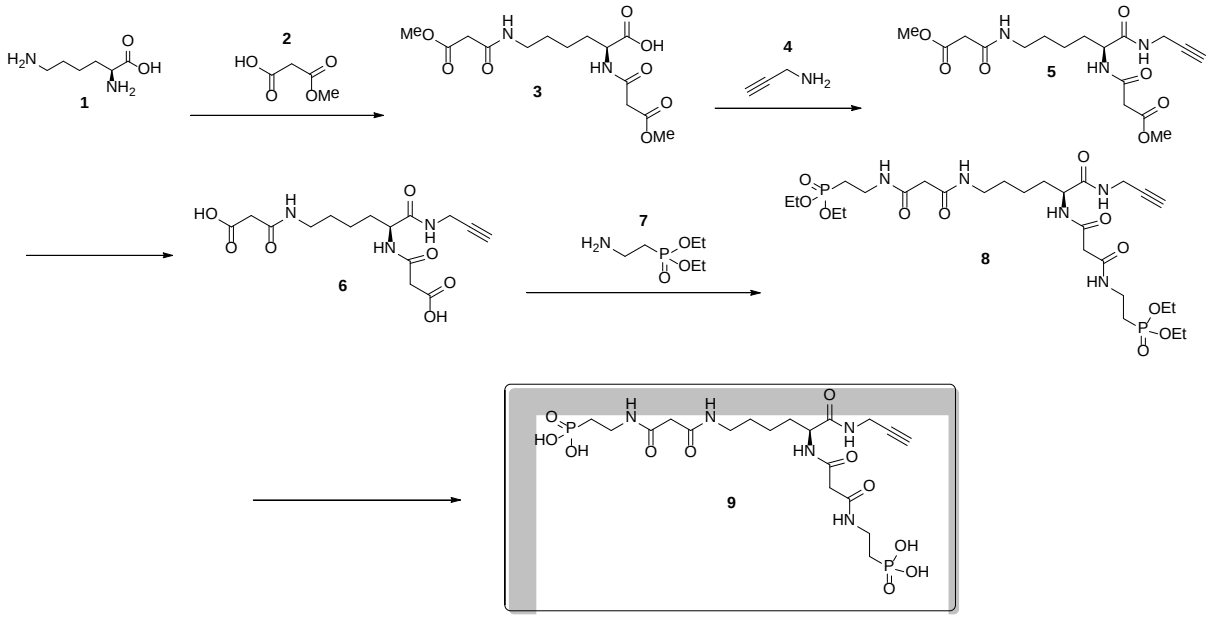

Scheme 1. Proposed synthetic route from L-lysine to the final phosphonic acid dendron

First, 2-(methoxycarbonyl)acetic acid **2** is coupled to L-lysine **1** [32]. The resulting diamide **3** is then reacted with 2-propynyl amine **4** via an amide coupling reaction to give triamide alkyne **5**. After basic deprotection of the methyl esters, diacid alkyne **6** is coupled with diethyl (2-aminoethyl)phosphonate **7** to yield ethylated diphosphonate **8**, which results in the desired diphosphonate **9** after deprotection of the ethyl esters [35].

Product **9** is the **G1** dendron. Further generations of this dendron can be synthesised by using the aza-Michael addition to introduce additional repeats to L-lysine **1**, which is shown in Scheme 2.

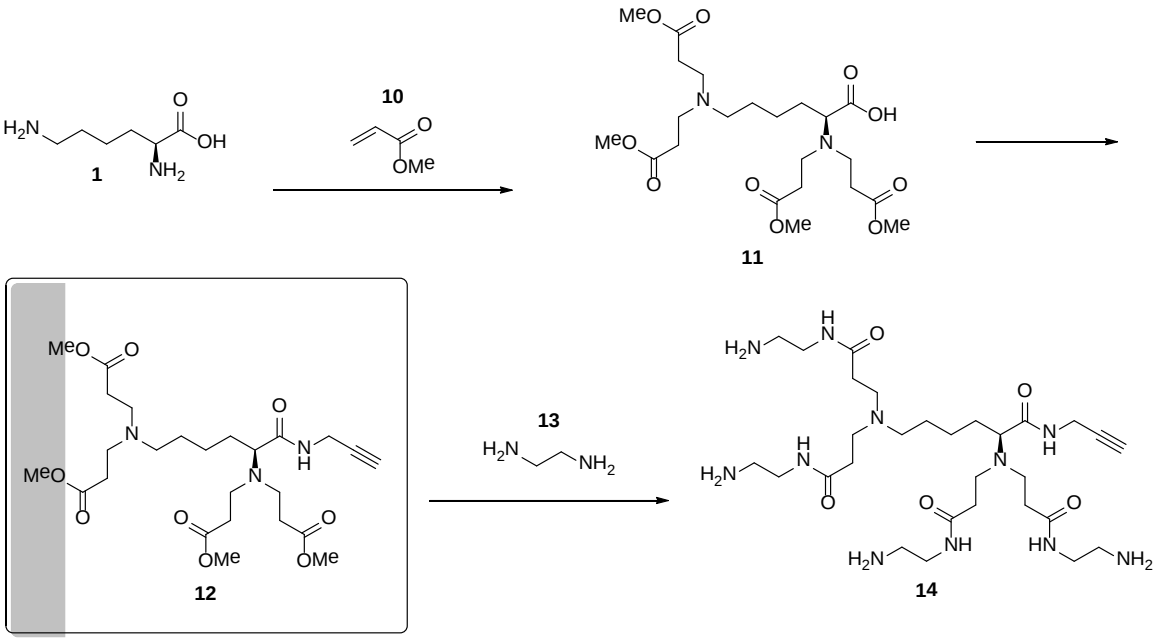

Scheme 2. Proposed synthetic route to the G2 dendron and further

L-lysine **1** is reacted with methyl acrylate **10** via an aza-Michael addition to give tetramethyl ester **11**, which is then coupled with 2-propynyl amine **4** to give tetra-acid alkyne **12**. This compound can then react via aminolysis with diethyl (2-aminoethyl)phosphonate **7** to yield the **G2** dendron, or with ethane-1,2-diamine **13** to give penta-amide alkyne **14**. The aza-Michael addition and the other steps described above can then be repeated on this compound to create further generations of the dendron.

During the synthesis, the purified products were verified by thin-layer chromatography (TLC), mass spectrometry (MS) and nuclear magnetic resonance (NMR). These results and the experimental procedures of all performed reactions can be found in the Supporting Information.

Results and Discussion

Amide coupling

In an effort to yield diamide **3**, methyl potassium malonate **15** was reacted with L-lysine in the presence of carbonyldiimidazole (CDI) under solvent-free conditions, as depicted in Scheme 3.

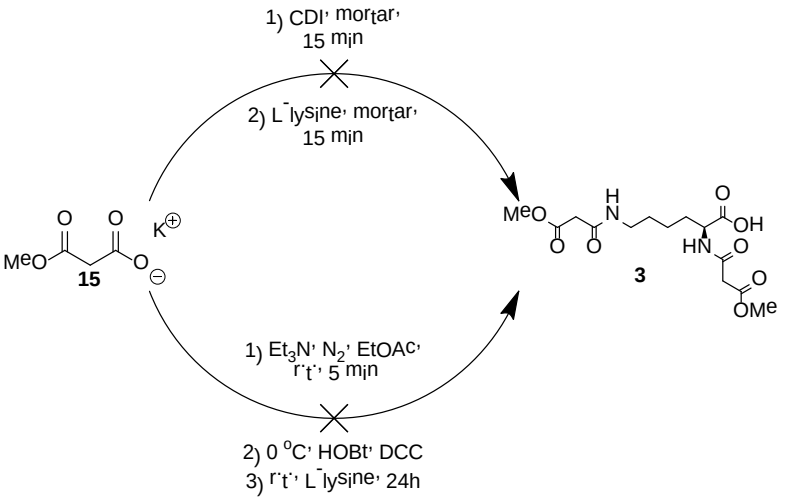

Scheme 3. Coupling reactions with methyl potassium malonate

While it is usually easy to see if a coupling reaction with CDI is proceeding by monitoring the liberation of CO_2, which is formed as the CDI reacts, during this reaction no CO_2 liberation was observed. This might have been caused by the fact that both methyl potassium malonate and CDI are solids and therefore the escape of CO_2 is very difficult to see with the naked eye. When the L-lysine was added, the mixture changed to a paste. However, after the procedure was completed, MS analysis showed no indication of a successful reaction, but only evidence of a reaction between CDI and L-lysine. The MS spectrum is shown in Figure 3.

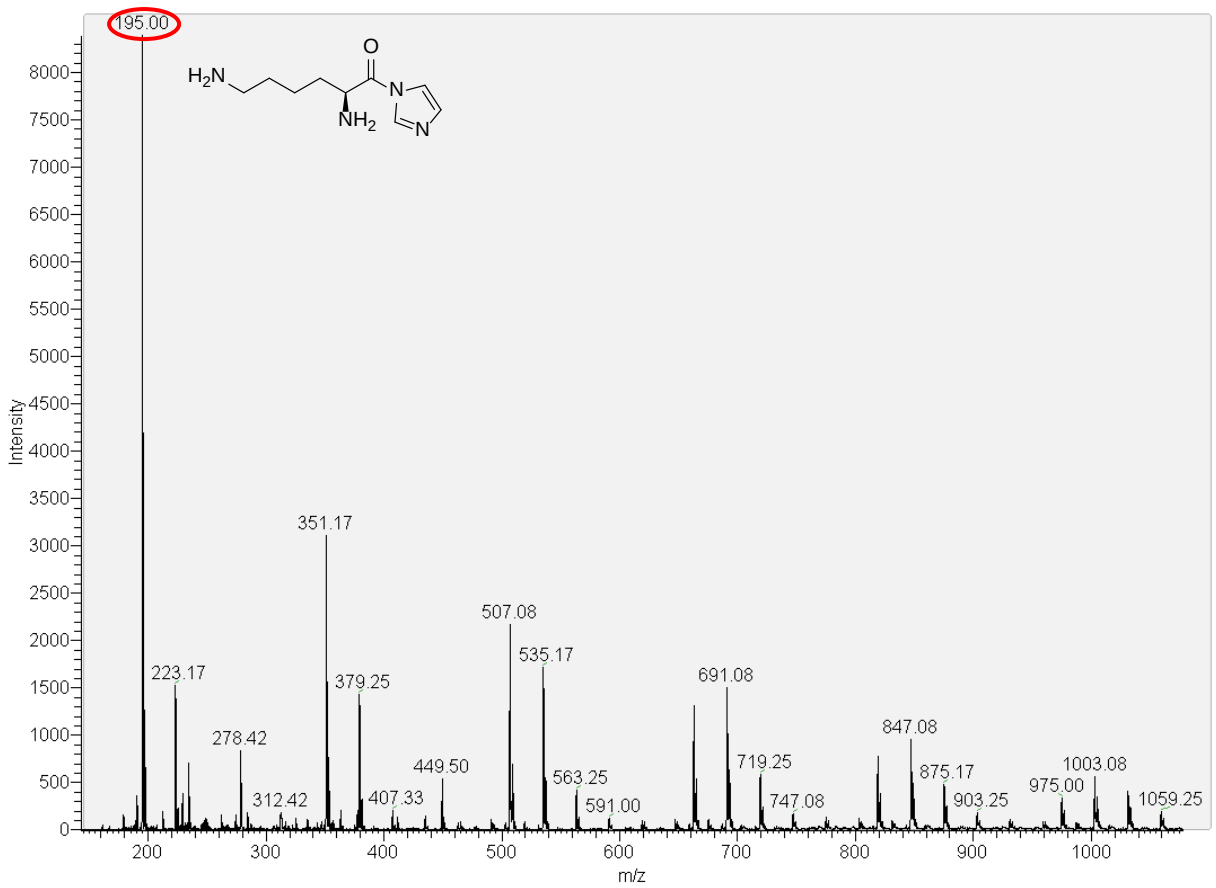

Figure 3. MS spectrum of the CDI-mediated amide coupling reaction with L-lysine and potassium methyl malonate. The structure of the product of the reaction between CDI and L-lysine, which corresponds to the marked $[M-H]^-$ adduct ion peak at m/z = 195.00, is shown.

A second attempt was made, using triethylamine (Et_3N), hydroxybenzotriazole (HOBt) and *N,N'*-dicylcohexylcarbodiimide (DCC) under a nitrogen atmosphere (Scheme 3). This reaction also failed to show signs that any conversion had taken place.

While both reactions failed to yield the desired product, indications suggest that this was caused by the fact that the added malonate is a salt and not a free organic compound. The fact that the reaction mixture of the CDI coupling changed from a mixture of solids to a paste is a strong indication that the CDI reacted with the L-lysine when it was added, which is confirmed by the MS data. This would implicate that the CDI could not react with the malonate salt, while it is known that CDI reacts readily with free carboxylic acid groups and even aqueous solutions of amino acid salts [36]. Study of the collected literature on CDI-mediated amidation suggests that under solvent-free conditions, CDI can only successfully react with free carboxylic acids [32, 33]. This is probably because protons are needed in the formation of the imidazole by-product. Therefore the reaction will not be able to succeed without them, as is the case when using a carboxylic acid salt like methyl potassium malonate under solvent-free conditions.

Because the coupling reaction between malonate and L-lysine might still be feasible if the malonate was added as the free organic compound or as an aqueous solution, the synthetic route proposed in Scheme 1 could still be viable.

Aza-Michael addition

Bi-adduct – Generation 1 dendron

To compensate for the fact that the amide coupling of the planned synthetic route did not succeed, a workaround route was devised based on the planned aza-Michael addition step, shown in Scheme 2. By performing the aza-Michael addition directly on L-lysine, the unsuccessful coupling reaction could be bypassed, resulting in the synthesis of **G1** dendron **22**. The adjusted synthetic route is shown in Scheme 4.

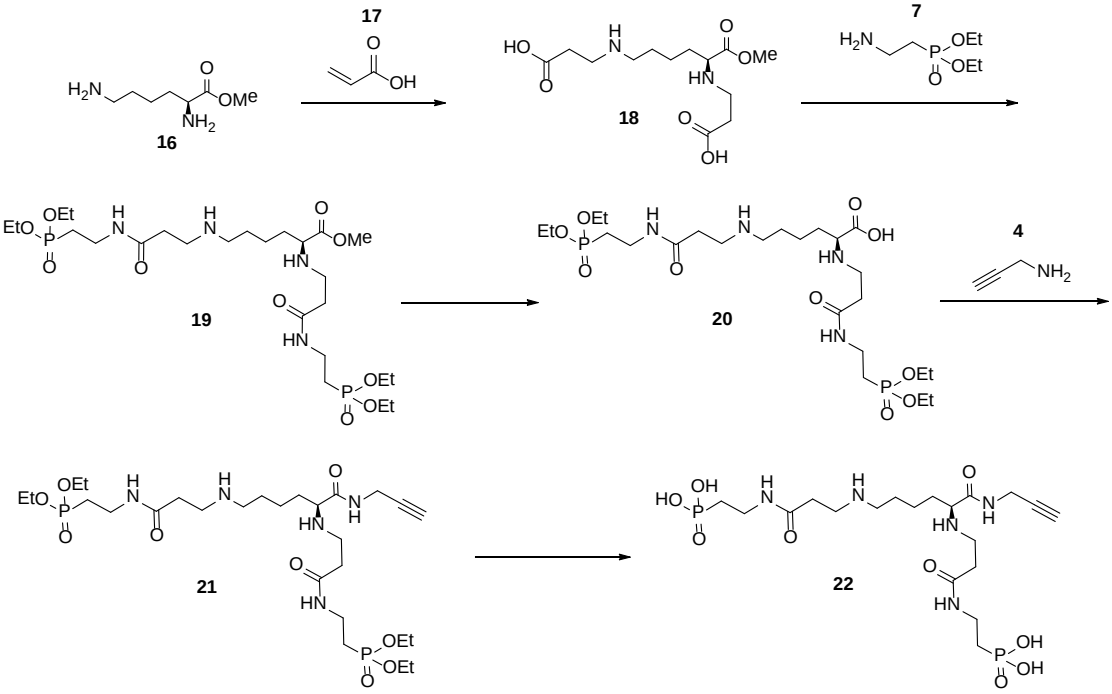

Scheme 4. Proposed workaround pathway using the aza-Michael addition

First, L-lysine methyl ester **16** is reacted with acrylic acid **17** using an aza-Michael addition. According to literature, performing this reaction in water at 70 °C can ensure this addition only occurs once on the available amines [37]. The resulting diacid **18** is then coupled to diethyl (2-aminoethyl)phosphonate **7** via an amide coupling reaction to yield diphosphonate **19**. Subsequent deprotection of the methyl ester gives rise to diphosphonate acid **20**, which is then coupled to 2-propynyl amine **4** via an amide coupling reaction to yield diphosphonate alkyne **21**. Finally, deprotection of the ethyl esters on the phosphonate tails results in the **G1** dendron **22**.

In a first attempt, depicted in Scheme 5, L-lysine methyl ester **16** was mixed with acrylic acid **17** in water and stirred for 4 days at 70 °C in an attempt to create diacid **18**.

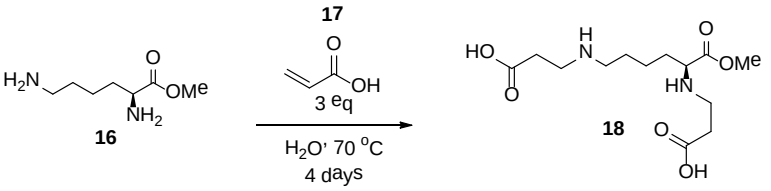

Scheme 5. Selective aza-Michael addition with L-lysine methyl ester and acrylic acid

However, MS analysis of the resulting reaction mixture indicated that, although diacid **18** was present, there was also evidence the methyl ester of the compound had been partially hydrolysed. This can be seen in Figure 4 and Table 1.

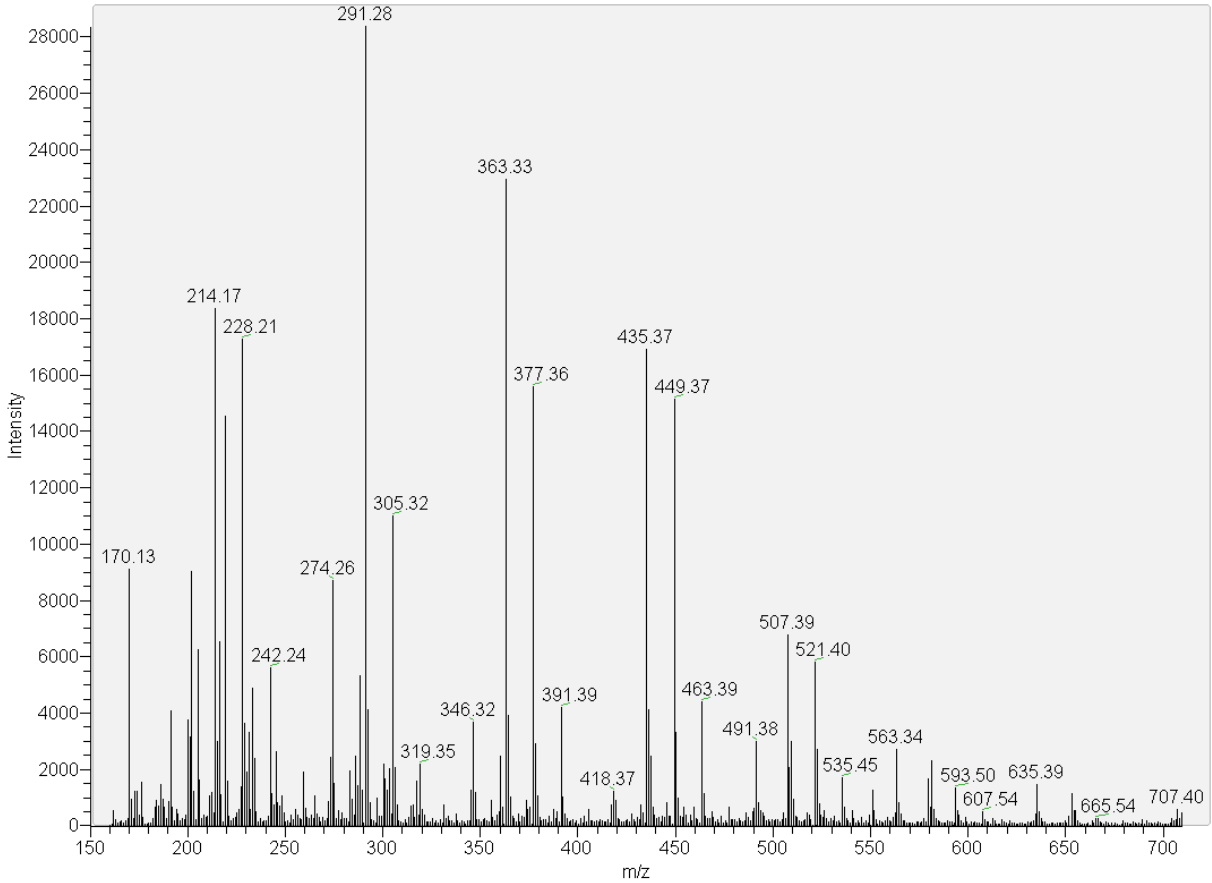

Figure 4. MS spectrum of the Michael addition reaction with L-lysine methyl ester and acrylic acid

Table 1. Peak analysis of the MS spectrum of the Michael addition with L-lysine methyl ester and acrylic acid. All peaks are $[M+H]^+$ adduct ions.

m/z	Compound
291.28	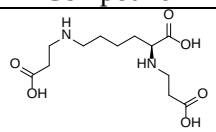
305.32	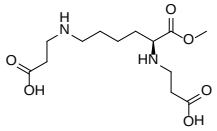
363.33	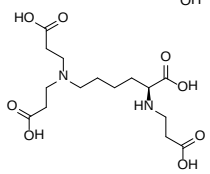
377.36	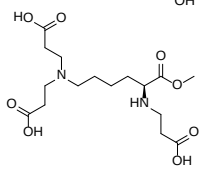

435.37	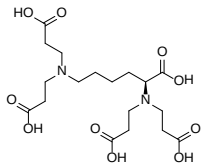
449.37	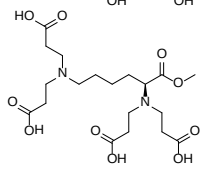
507.39	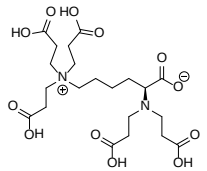
521.40	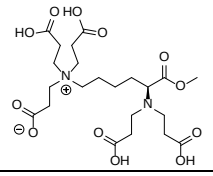

As can be seen in Table 1, the MS spectrum shows evidence that the aza-Michael addition was not selective. Apart from the expected diacid **18**, the reaction also created tri-adducts, tetra-adducts and even a zwitterionic penta-adduct. More importantly, the spectrum also shows evidence of hydrolysis of the methyl ester in all these products. This would lead to a loss of selectivity between the carboxylic acid groups of the acrylate tails and the group of L-lysine in the next step of the synthesis and prevent the creation of diphosphonate **19**. Therefore, another procedure had to be found.

Using a milder procedure devised by Ranu et al. [38] and depicted in Scheme 6, the reaction was performed using L-lysine **1** and methyl acrylate **12**, which would result in the creation of the dimethyl ester **23**.

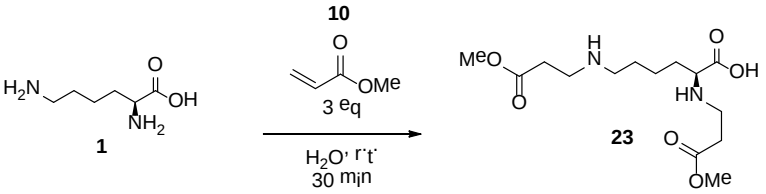

Scheme 6. Milder procedure for the selective aza-Michael addition with L-lysine and methyl acrylate based on the research of Ranu et al.

Ranu et al. speculate that it is the dual action of water, which coordinates the amine to the carbonyl oxygen atom of the α,β-unsaturated carbonyl of methyl acrylate via hydrogen bonding and thereby activates both the amine and the conjugated alkene, that speeds up the reaction, producing good yields in less than one hour at room temperature. Additional to this, they report that the observed reactions with primary amines only produced mono-addition products.

Based on the procedure used in literature, L-lysine **1** was mixed with methyl acrylate **10** in water and stirred at room temperature for 30 minutes before the mixture was analysed by MS. The resulting information is shown in Figure 5 and Table 2.

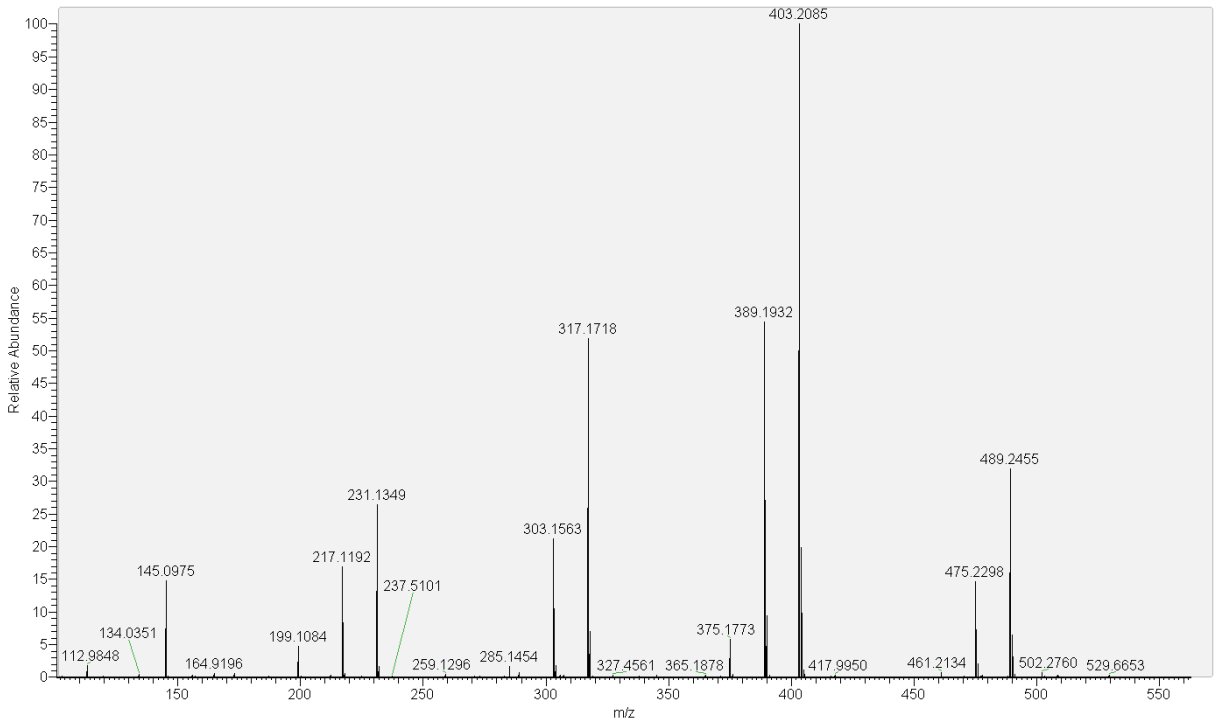

Figure 5. MS spectrum of the aza-Michael addition with L-lysine and methyl acrylate at room temperature

Table 2. Peak analysis of the MS spectrum of the Michael addition with L-lysine and methyl acrylate at room temperature. All peaks are [M-H]$^-$ adduct ions.

m/z	Compound
145.0975	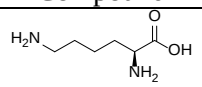
217.1192	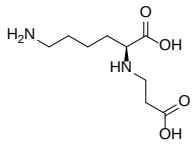
231.1349	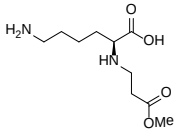
303.1563	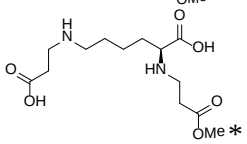 *
317.1718	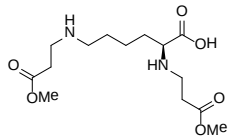
375.1773	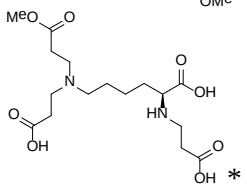 *

389.1932	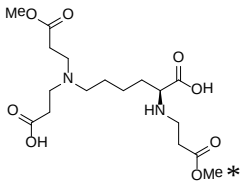
403.2085	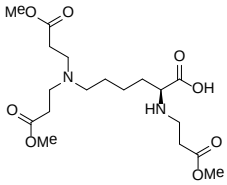
475.2296	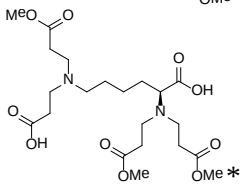
489.2455	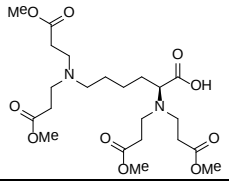

* In the case of compounds with multiple methyl ester groups, the structures of the hydrolysed compounds shown are only an indication and have not been proven.

As can be seen from the spectrum information, the reaction proved to be non-selective, indicated by the presence of tri- and tetra-adducts. Furthermore, hydrolysis of the methyl esters has again taken place and is already taking place when the conversion of the reaction is incomplete, as indicated by the presence of L-lysine starting material and mono-adduct.

In an effort to stop the hydrolysis of the methyl esters and increase the selectivity of the reaction, the reaction was repeated, but at 0 °C. The reaction, shown in Scheme 7, was then stirred for 40 minutes and samples were taken for MS analysis every 20 minutes.

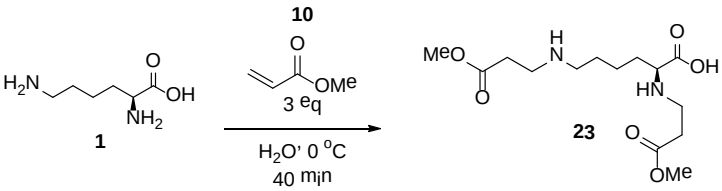

Scheme 7. Aza-Michael addition with L-lysine and methyl acrylate at 0 °C

The resulting spectra can be found in the Supporting Information (Figure 29 & Figure 30) and indicate that hydrolysis of the methyl esters is indeed prevented using the new reaction conditions. However, they also show that 20 minutes into the reaction, tri-adduct is already forming and after 40 minutes, the presence of tetra-adduct is also visible.

In order to stop the formation of tri-adduct, the reaction was repeated using the same reaction conditions, but with tert-butyl acrylate **24** instead of methyl acrylate (Scheme 8).

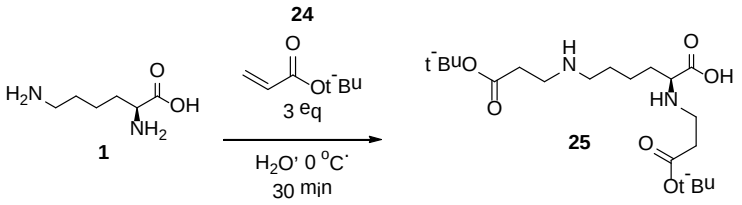

Scheme 8. Aza-Michael addition with L-lysine and tert-butyl acrylate at 0 °C

It was speculated that the introduction of more steric hindrance would make the formation of the tri-adduct more difficult, resulting in the tert-butyl protected L-lysine **25** as the major reaction product. Therefore, the reaction was stirred for 30 minutes at 0 °C and the mixture was then analysed by MS. The spectrum is shown in Figure 6.

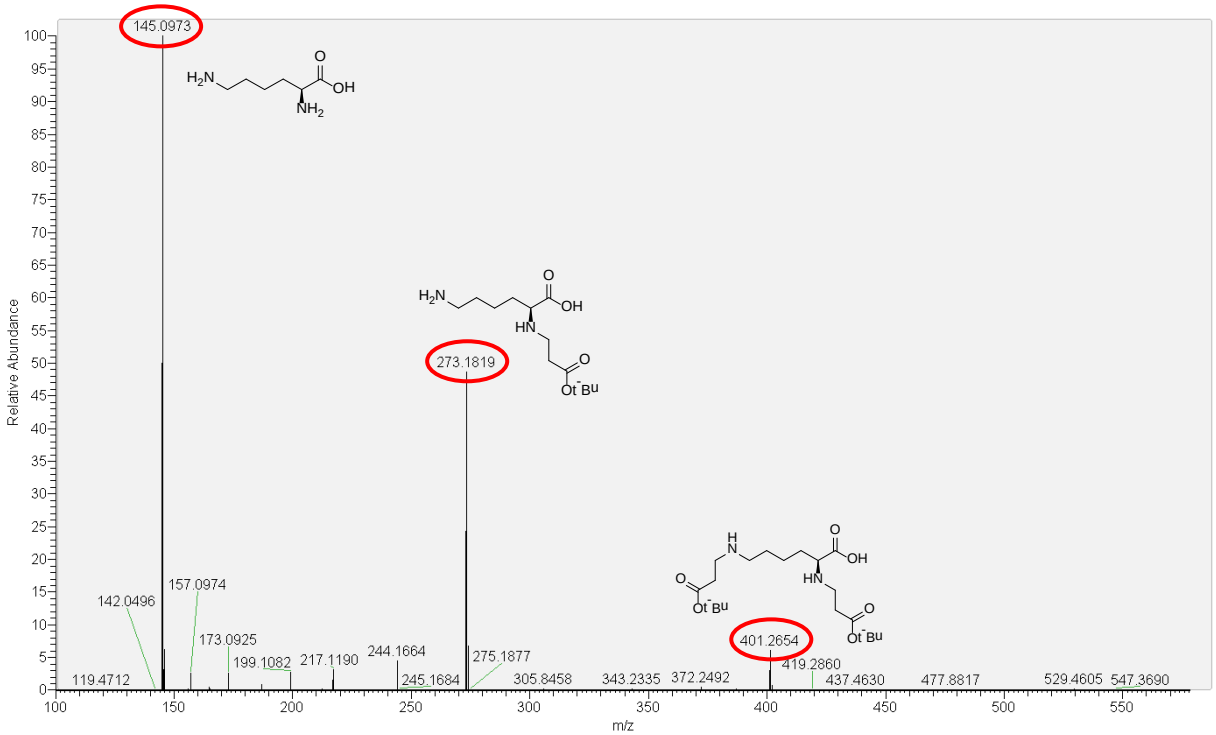

Figure 6. MS spectrum of the aza-Michael addition with L-lysine and tert-butyl acrylate at 0 °C after 30 minutes. All marked peaks are $[M-H]^-$ adduct ions and structures of the corresponding compounds are shown.

The MS results indicate that the increased steric hindrance also influences the speed of the formation of the mono- and bi-adduct. However, because of time constraint, the reaction could not be followed any longer.

The reaction was repeated using the same conditions, this time with 2 equivalents of tert-butyl acrylate instead of the previously used 3 equivalents in hopes to even better control the reaction. Samples were taken every 20 minutes for 5 hours to be analysed by MS. The results are shown in Figure 7 and Table 3.

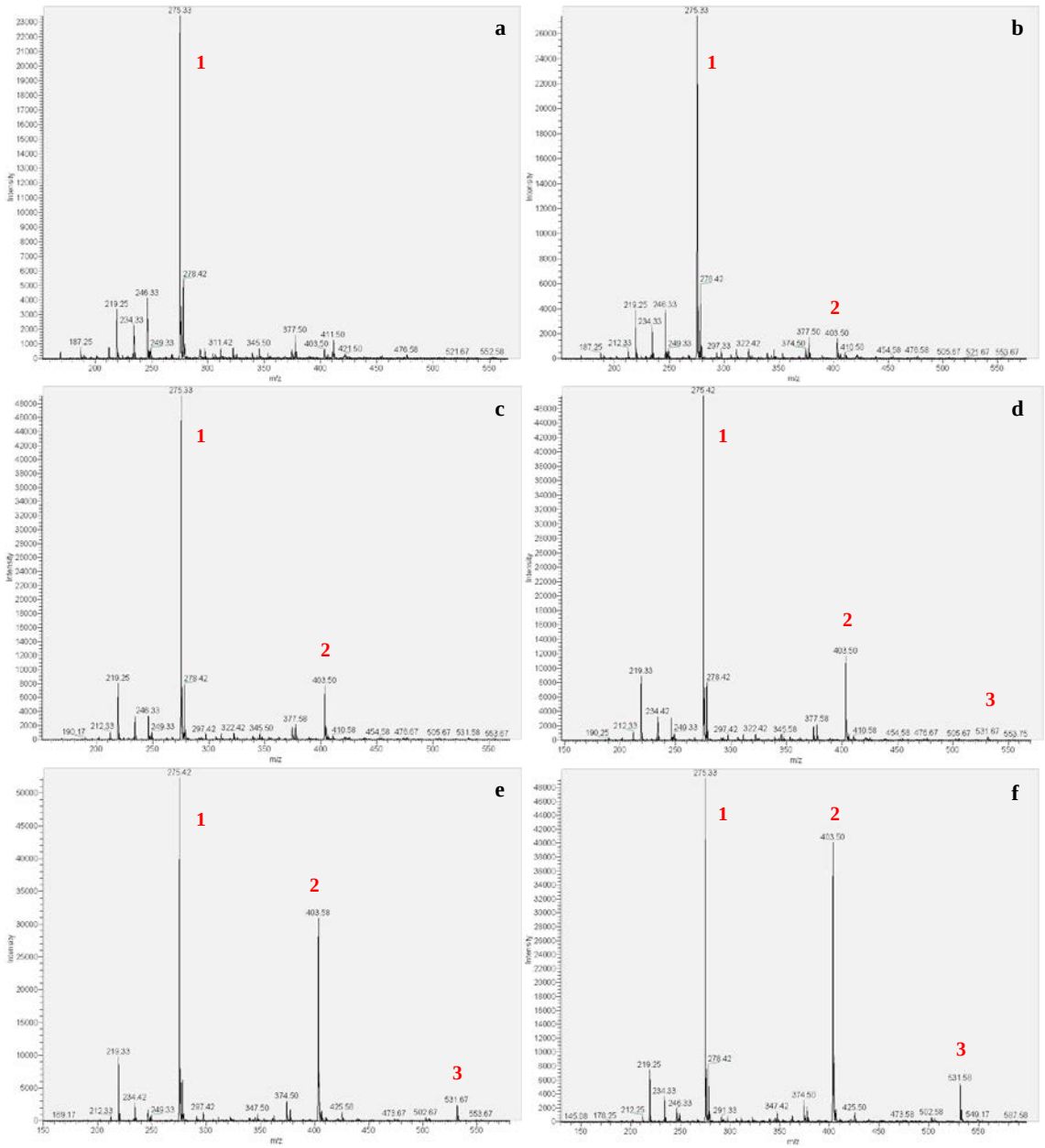

Figure 7. MS spectra of the aza-Michael reaction between tert-butyl acrylate and L-lysine at 0 °C. Depicted are the samples taken at a) 40 min b) 80 min c) 120 min d) 160 min e) 220 min and f) 320 min. The numbered peaks are analysed in the table below.

Table 3. Peak analysis of the MS spectra of the aza-Michael reaction between tert-butyl acrylate and L-lysine at 0 °C. All peaks are $[M+H]^+$ adduct ions.

Number	m/z	Compound
1	275.33 – 273.42	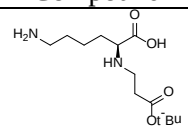
2	403.50 – 403.88	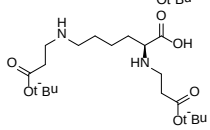
3	531.58 – 531.67	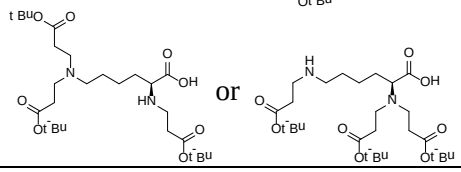

As can be seen, the tri-adduct is already being formed before all of the mono-adduct has reacted to bi-adduct, indicating that the reaction speed of the aza-Michael addition on a secondary amine could be faster than the addition on a primary amine.

In a final effort to use the aza-Michael addition in the production of the desired bi-adduct, the first experiment with tert-butyl acrylate was repeated with L-lysine methyl ester **16** instead of L-lysine **1** to give compound **26**. The reaction is shown in Scheme 9.

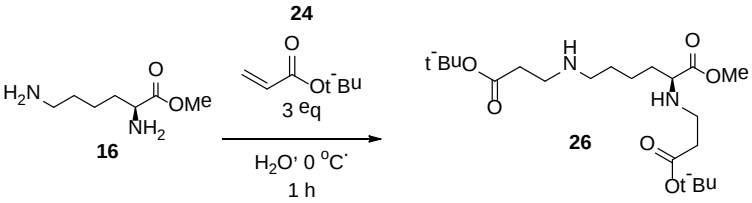

Scheme 9. Aza-Michael addition of L-lysine methyl ester and tert-butyl acrylate at 0 °C

The reaction was stirred for 1 hour at 0 °C and samples were taken every 20 minutes for MS analysis. The MS spectra can be found in Figure 31 & Figure 32 in the Supporting Information.

As can be seen in the MS spectra of this reaction, no product was formed. This might have been caused by the absence of a free carboxylic acid group, which was always present during the other performed aza-Michael additions, either in the form of the carboxylic acid group of L-lysine or the group of acrylic acid. As has been shown in previous research, protons catalyse the Michael addition [39, 40], therefore the absence of a free carboxylic acid group during this reaction might explain why no products were formed. This was however not investigated further.

An overview of all the aza-Michael addition reactions that were performed is shown in Scheme 10.

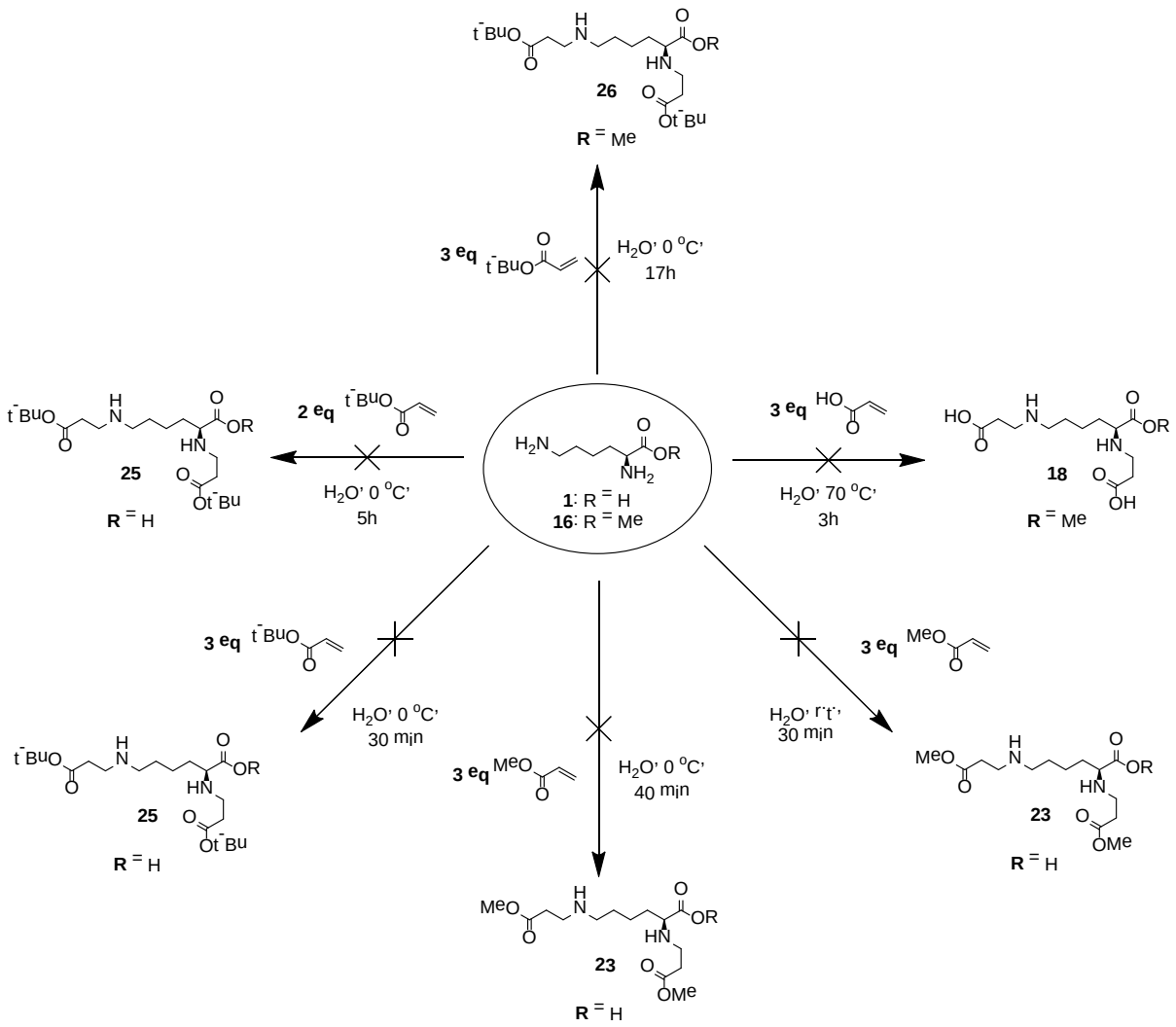

Scheme 10. An overview of all performed aza-Michael reactions

Tetra-adduct – Generation 2 dendron

Although the selective synthesis of a **G1** PAMAM dendron using the aza-Michael addition on L-lysine proved unsuccessful, the indication that tri-adducts were formed very fast during the reactions indicated that the formation of a **G2** dendron might be possible in just one step. Based on these observations and on research by Lind et al. [40, 41], another synthetic route was devised to produce this **G2** dendron **31**, which is shown in Scheme 11. This scheme uses the same steps as Scheme 4, but in a different order.

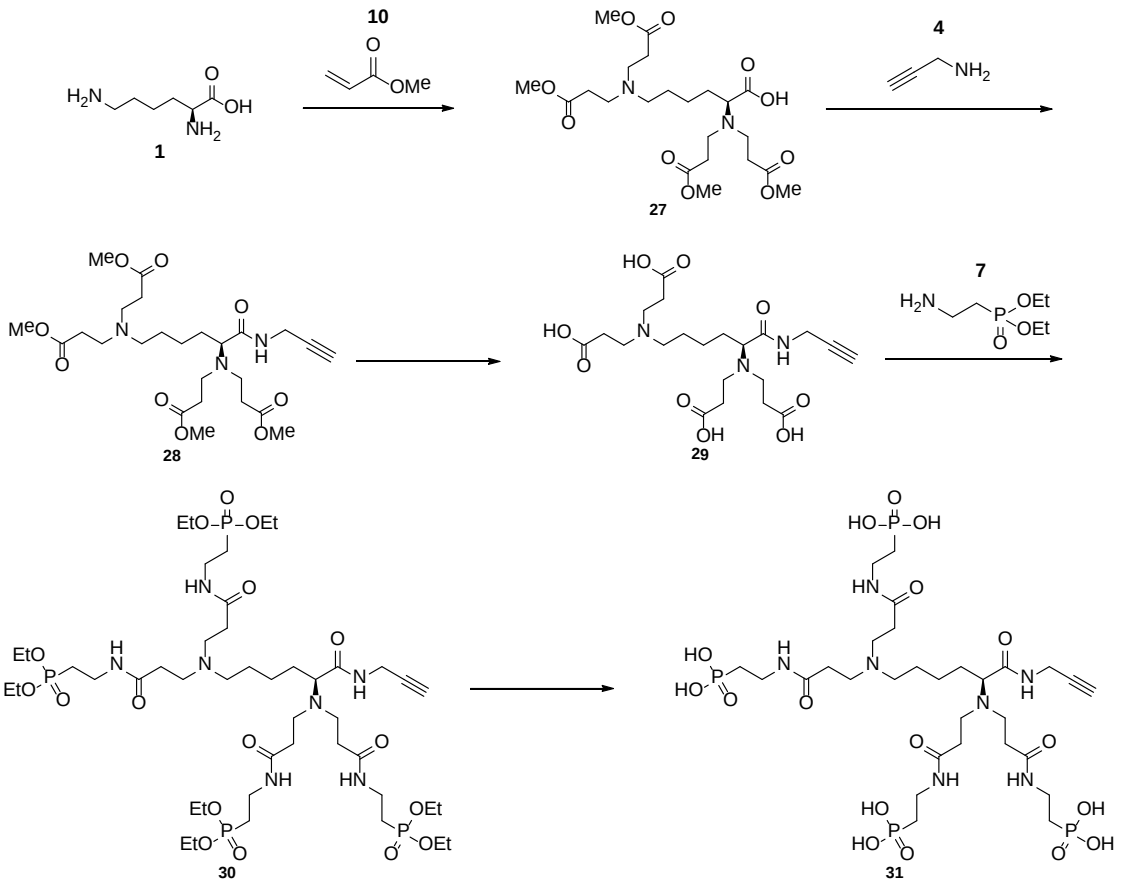

Scheme 11. Proposed synthetic pathway of the generation 2 dendron using the aza-Michael addition

First an aza-Michael addition is performed with L-lysine **1** and methyl acrylate **10** to create the tetramethyl ester **27**. To this compound is then coupled 2-propynyl amine **4** via an amide coupling reaction to give alkyne **28**. Subsequent deprotection of the methyl esters yields tetra-acid alkyne **29**. Diethyl (2-aminoethyl)phosphonate **7** is then coupled to this compound using an amide coupling reaction, which gives the tetraphosphonate alkyne **30**. Finally, deprotection of the ethyl esters yields the finished **G2** phosphonate dendron.

To start the synthesis of the **G2** dendron, L-lysine **1**, sodium hydroxide (NaOH) and methyl acrylate **10** were added to methanol (MeOH) and the mixture was stirred and refluxed for 2 days, as shown in Scheme 12. MS analysis of the reaction mixture indicates that the reaction was successful, as can be seen in Figure 8 and Table 4. The MS spectrum of the negative mode measurement can be found in Figure 33 and Table 8 of the Supporting Information.

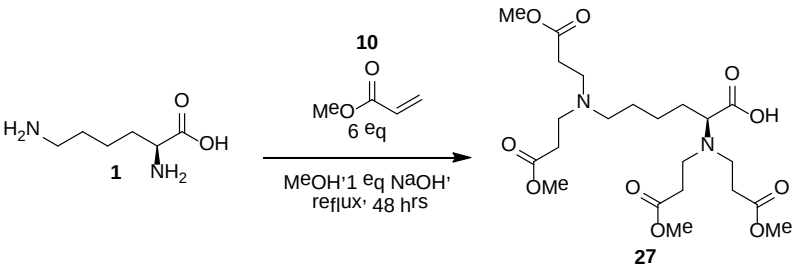

Scheme 12. Aza-Michael addition with L-lysine and acrylic acid based on research by Lind et al.

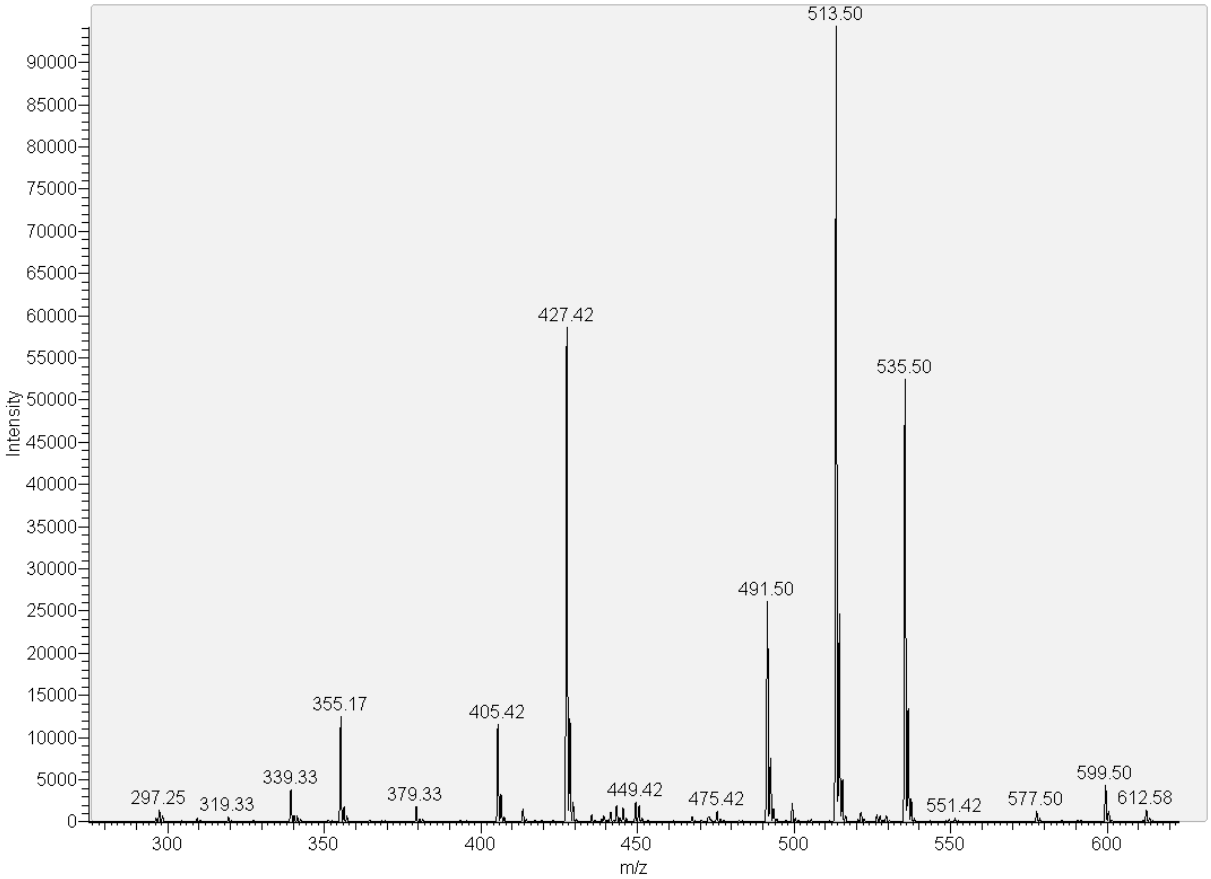

Figure 8. MS spectrum of the aza-Michael addition with L-lysine and methyl acrylate after 48 hours.

Table 4. Peak analysis of the MS spectrum of the aza-Michael addition with L-lysine and methyl acrylate after 48 hours.

m/z	Adduct ion	Compound
405.42	$[M+H]^+$	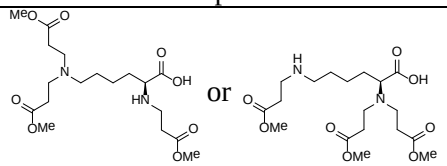
427.42	$[M+Na]^+$	
491.50	$[M+H]^+$	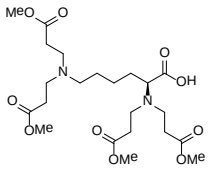
513.50	$[M+Na]^+$	
535.50	$[M+2Na-H]^+$	

Both MS spectra show the presence of the desired tetramethyl ester **27**, but also tri-adducts and small amounts of methyl ester hydrolysis. The extraction was performed and an attempt was made to purify the mixture following the experimental procedure reported by Lind et al. [41], but this presented a problem.

While Lind et al. report the use of SiO_2 column chromatography to finally isolate the tetra-adduct **27** or similar compounds, attempts to reproduce this feat with the reported eluent, other eluents and changing to alumina as the solid phase were unsuccessful in separating the tetra-adduct **27** from tri-adducts **28a** and/or **28b** (Figure 9) that were also formed during the reaction.

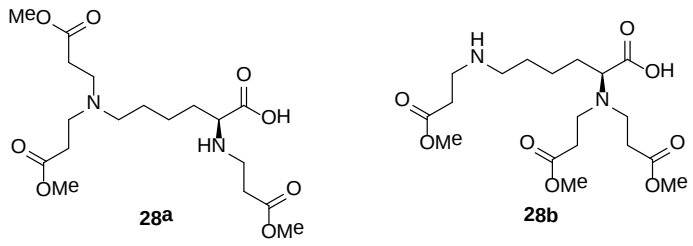

Figure 9. Two possible structures of the tri-adduct of the aza-Michael addition with L-lysine and methyl acrylate

Eventually, column chromatography on reverse phase C_{18} silica proved to be effective in separating the tri-adduct and tetra-adduct from most of the contaminants, but not from each other. NMR analysis of the resulting mixture is shown in Figure 10.

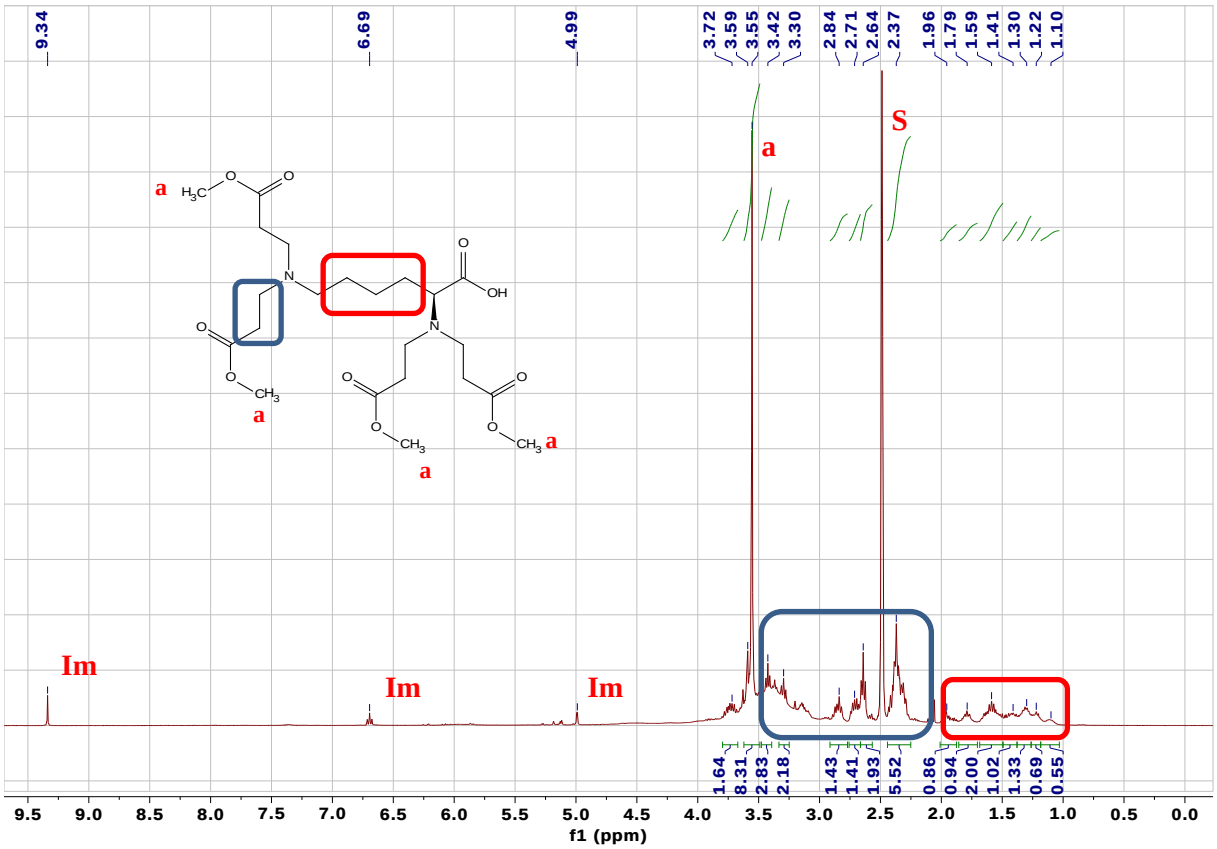

Figure 10. ^{1}H NMR spectrum of the tri- and tetra-adduct mixture after reverse phase column purification, the structure of the tetra-adduct 27 is shown. Marked peaks are as follows: impurities (Im) and solvent (S). Obtained in DMSO-d_6.

The NMR spectrum shows several peaks (blue area) which correspond to all products of the aza-Michael addition observed in the MS spectrum. Getting specific information about the ratio between tri- and tetra-adduct becomes very difficult, as the peaks of the different structures have significant overlap in the marked area, making the assignment of peaks problematic. However, the ratio between the methyl ester signal (**a**) and the signal of the L-lysine backbone (red area) the presence of products with more than two additions.

An experiment was performed to see if the reaction could by driven to fully convert all of the tri-adduct to tetra-adduct given enough time, but MS analysis of the obtained reaction mixture indicates that this will not work or take a very long time (>12 days). The MS spectrum of an aza-Michael addition that was left to react for 11 days can be seen in Figure 11. A full analysis of all peaks can be found in Table 9 in the Supporting Information.

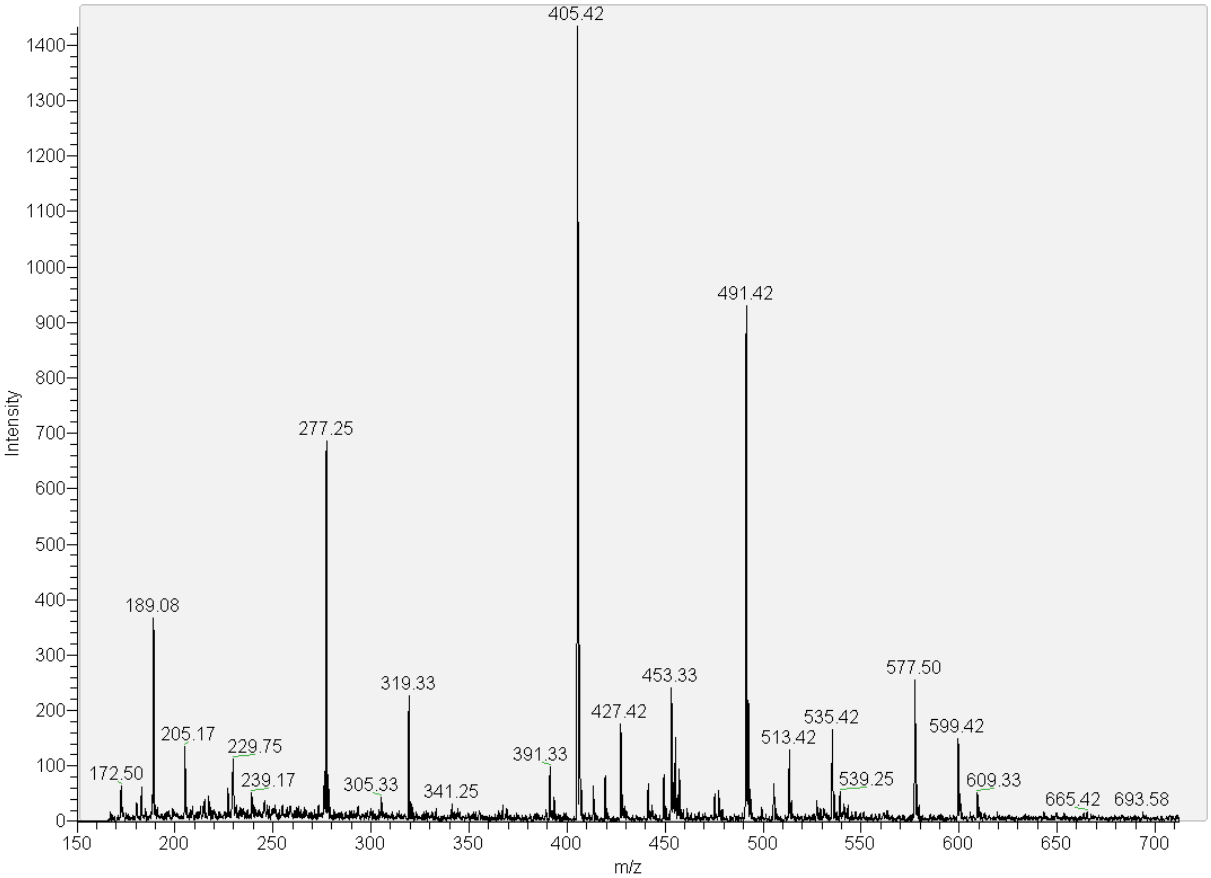

Figure 11. MS spectrum of an aza-Michael addition of methyl acrylate and L-lysine, reacted for 11 days. The peaks at m/z = 405.42 and 491.42 belong to the $[M+H]^+$ adduct ion of the tri-adduct and the tetra-adduct respectively.

The MS spectrum shows that even after 11 days, not all tri-adduct has been converted to tetra-adduct, even though some of the tetra-adduct has been converted to a penta-adduct. These MS and NMR results and the yield reported by Lind et al. (48.8%) seem to indicate that this reaction achieves equilibrium at some point, preventing the yield of the reaction from increasing. The obtained crude mixture of both compounds was used in further experiments.

To continue on the synthetic route toward the finished **G2** dendron, an attempt was made to modify the free carboxylic acid group of both the tri- and tetra-adducts. After this modification the separation between the two compounds might improve. The combination of a free carboxylic acid and two tertiary amines (or a secondary and a tertiary amine in the case of the tri-adducts) made it very difficult

to find an eluent mixture with the right pH to successfully perform column chromatography using unmodified SiO_2. An eluent mixture with a higher pH would be a good option for separation after the modification, as the acidic nature of silica would be neutralised, preventing the protonation of the amines and thereby the formation of salts with the compound.

To this end, the crude mixture of tri- and tetra-adduct was reacted under solvent-free conditions with CDI, after which allyl amine **29** was added. Just like 2-propynyl amine **4**, the addition of a double bond could be used to 'click' the finished dendron to a second dendron, completing the 'Janus' dendrimer, but a small amount of the resulting vinyl product **30** would also be easier to observe in a ^1H NMR spectrum. This is because the protons of the vinyl group would have peaks in an otherwise empty part of the spectrum (between 5 and 6 ppm), while the peaks of the acetylene group would be situated in the part of the spectrum also containing the peaks of the CH_2-groups from the methyl ester tails (between 3 and 4 ppm). The reaction is depicted in Scheme 13.

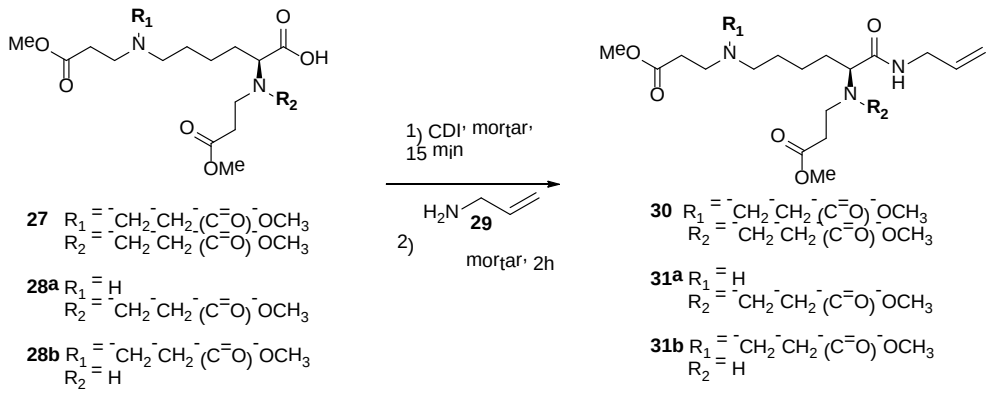

Scheme 13. Amide coupling reaction between the tetra-adduct and allyl amine

MS analysis of the resulting reaction mixture show indications that the reaction works as expected, as can be seen in Figure 12 and Table 5.

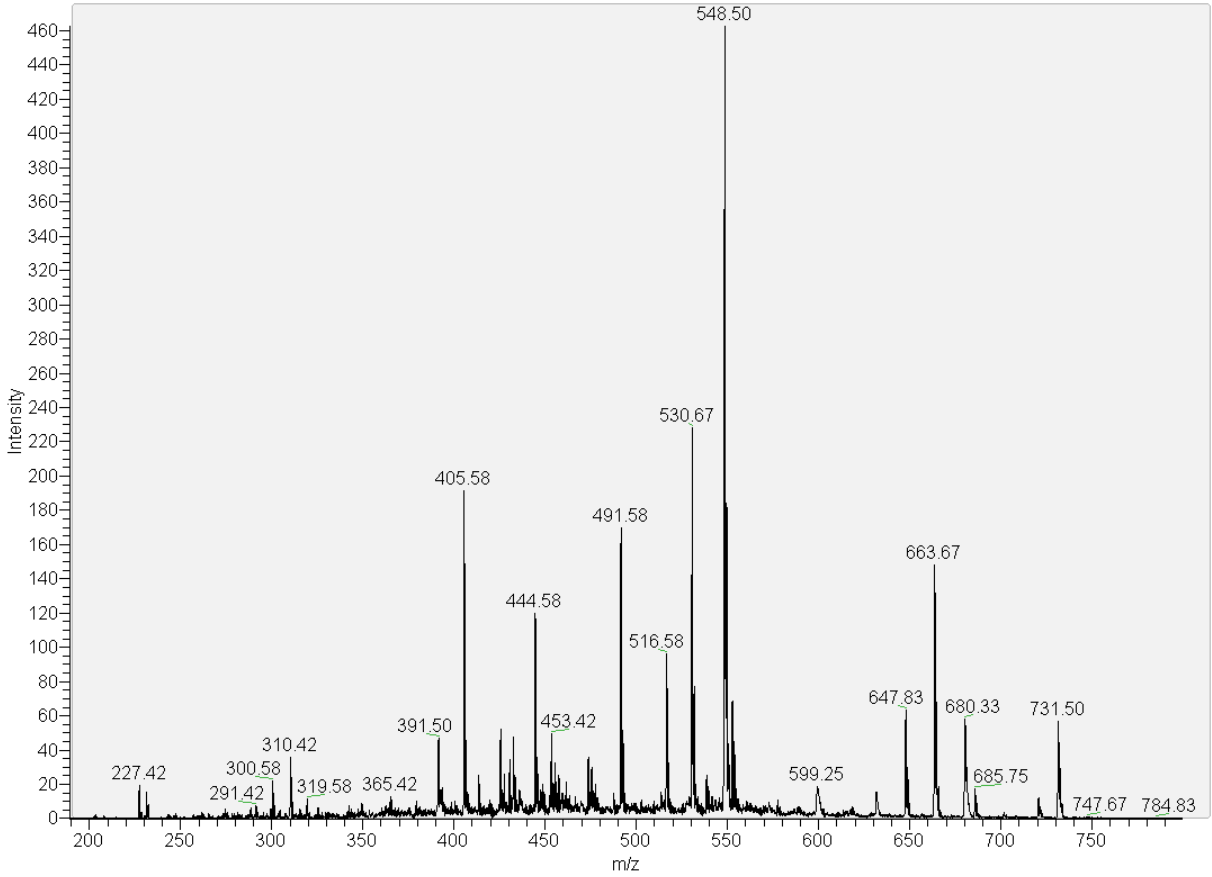

Figure 12. MS spectrum of the amide coupling reaction mixture between the tri-adduct/tetra-adduct mixture and allyl amine

Table 5. Peak analysis of the MS spectrum of the amide coupling reaction mixture between the tri-adduct/tetra-adduct mixture and allyl amine

m/z	Adduct ion	Compound
405.58	$[M+H]^+$	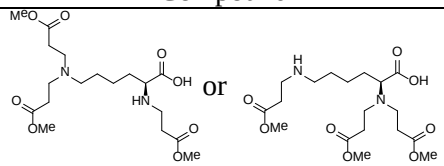 or
444.58	$[M+H]^+$	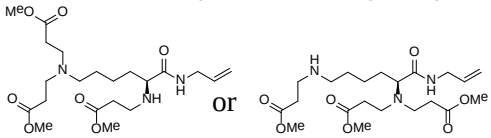 or
491.58	$[M+H]^+$	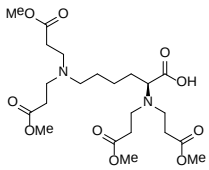
530.67	$[M+H]^+$	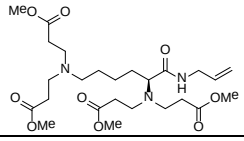
548.50	$[M+NH_4]^+$	

The MS spectrum shows that the reaction mixture still contains unreacted starting material in the form of the tetra-adduct **27** and the tri-adducts **28a**/**28b**. However, the presence of vinyl products **30** & **31a**/**31b** is also confirmed.

^{1}H NMR spectrum data of the crude reaction mixture, shown in Figure 13, also supports the MS result.

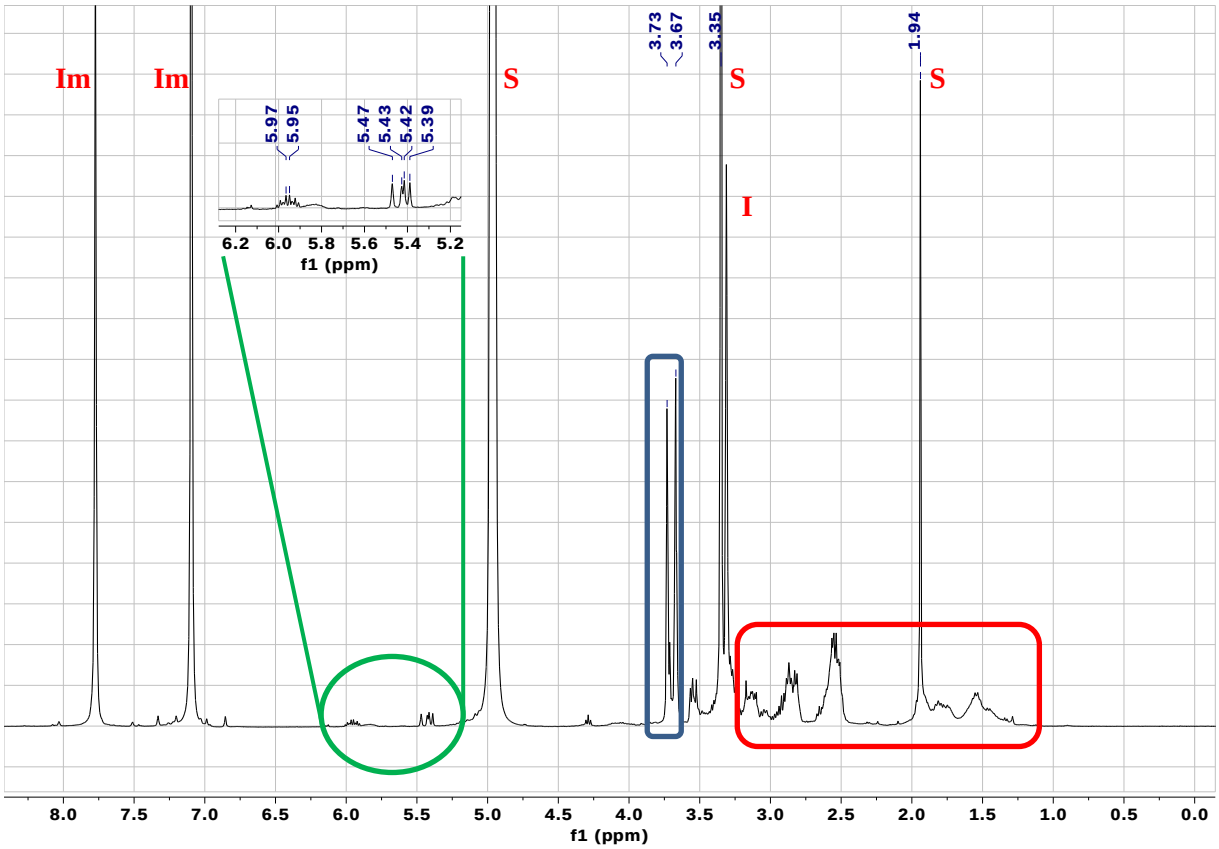

Figure 13. ^{1}H NMR spectrum of the CDI-induced amide coupling reaction mixture. Peaks are marked as follows: solvents (S), imidazole by-product (Im) and impurity (I). Obtained in CD_3OD.

From the ^{1}H NMR spectrum, several things can be observed. The peaks in the blue box represent signals from the methyl ester groups present in both the tri- and tetra-adduct starting material and the vinyl products, while the peaks in the red box are indicative for the L-lysine backbone and the CH_2-groups of the methyl ester tails.

The presence of imidazole shows that the CDI-induced coupling reaction is proceeding, which is further strengthened by the appearance of the peaks in the green circle. These peaks are representative of the vinyl group, which has been coupled to the tri- or tetra-adduct. The low signal strength of these peaks indicates that, although the reaction proceeds, the conversion is not very high. In short, both MS and NMR show that the CDI-mediated coupling reaction was successful, but the conversion of the reaction with the used reaction conditions was very low.

After a silica column purification using ethyl acetate (EtOAc)/MeOH at a ratio of 9:1 with 5% aqueous ammonia as the eluent, the resulting fraction was characterized by NMR using ^{1}H, ^{13}C, 2D Heteronuclear Multiple Bond Correlation (HMBC), 2D Heteronuclear Single Quantum Coherence and 2D Correlation Spectroscopy (COSY) measurements. These spectra and the corresponding tables can

be found in the Supporting Information (Figure 23-25 & Table 6-7). From the obtained NMR data, several conclusions can be drawn.

First, while the presence of the expected vinyl product **30** was proven in the crude reaction mixture, after the purification its presence cannot be confirmed with any certainty. While there are peaks in the ^{1}H NMR spectrum at 5.852 and around 5.193-5.069 ppm that are indicative of a vinyl group, there is no way to prove that this vinyl group is actually connected to the L-lysine backbone of the desired compound, as the peaks that are needed for this confirmation are missing from the obtained NMR spectra.

However, it is unlikely that these peaks are from the allyl amine, as this compound is very volatile and was likely evaporated in its entirety by the multiple and long usage of a rotary evaporator in the purification process. This strengthens the idea that these peaks belong to vinyl product **30**, although the size of the peaks and the absence of the peaks for the L-lysine backbone and the CH_2-groups of the methyl ester tails indicates that the amount of product present is even lower than in the crude mixture. It is therefore most likely that during the column purification, the vast majority of the desired product was not separated and was left on the column, probably because of incorrect interpretation of the obtained TLC results. However, MS analysis of the measured sample was not performed, preventing any definitive way of proving the matter.

Second, when all the information from the NMR spectra is combined, it indicates the presence of the compound **32** depicted in Figure 14. The observed peaks of this by-product in the ^{1}H spectrum, ^{13}C spectrum and the interactions of those peaks in the COSY, HMBC and HSQC correspond neatly with the predicted signal values.

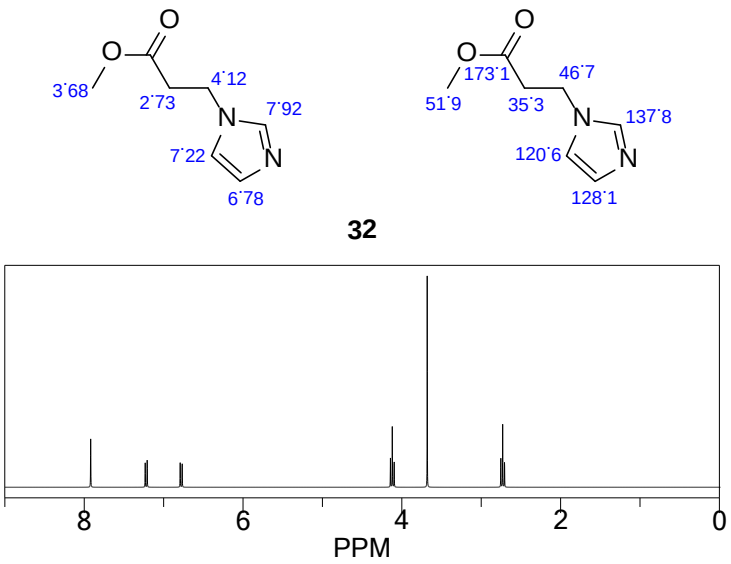

Figure 14. Structure, ^{1}H NMR spectrum prediction (left, bottom) and ^{13}C NMR prediction (right) of the main impurity of the column-purified amide coupling reaction product. NMR predictions were created in ChemBioDraw Ultra 2010.

A final piece of evidence that supports the presence of this particular impurity is given by the MS analysis of the reaction mixture during the column purification, shown in Figure 15.

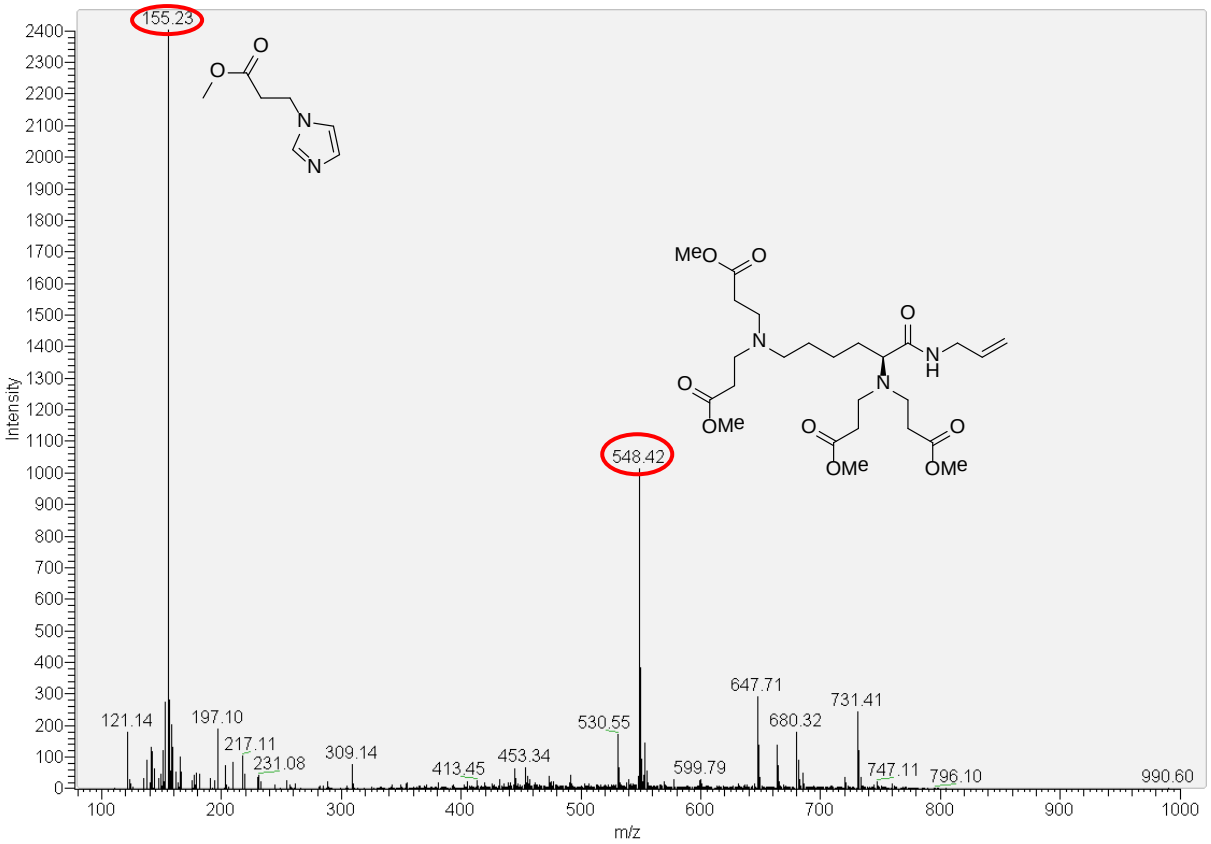

Figure 15. MS spectrum taken during the column purification of the amide coupling reaction mixture. The structures corresponding to the marked peaks at m/z = 155.23 ($[M+H]^+$) and 548.42 ($[M+NH_4]^+$) are shown.

The impurity is formed by the aza-Michael addition of imidazole, produced by the amide coupling with CDI, and methyl acrylate **12**. The presence of compound **32** indicates that not all the methyl acrylate had been removed from the tri- and tetra-adduct mixture used in the coupling reaction, which might also explain why there are two peaks for the methyl ester group in the ^{1}H NMR spectrum in Figure 13.

To prevent its presence in further iterations of the amide coupling reaction, repeated co-evaporations of the reaction mixture with MeOH could be used to make sure all methyl acrylate has been removed. This is driven by the fact that MeOH and methyl acrylate form a low-boiling azeotrope when mixed.

Thus, while MS and NMR analysis of the crude reaction mixture gives strong indications that the amide coupling reaction to produce vinyl compound **30** works, albeit at a very slow conversion rate, a final purified compound could not be isolated. Further optimisation and analysis of the reaction is therefore needed to make this reaction a viable way to produce the desired **G2** dendron.

Reductive amination

Since the aza-Michael addition proved to be impractical in selectively producing a **G1** dendron, another synthetic route was devised to facilitate this. This route is based on previous work performed by Medea Kosian, who used the same steps in the creation of a symmetric dendron based on 6-aminocaproic acid. Depicted in Scheme 14, it uses a reductive amination to ensure that only one phosphonate tail will be coupled to each amine, resulting in **G1** diphosphonate dendron **40**.

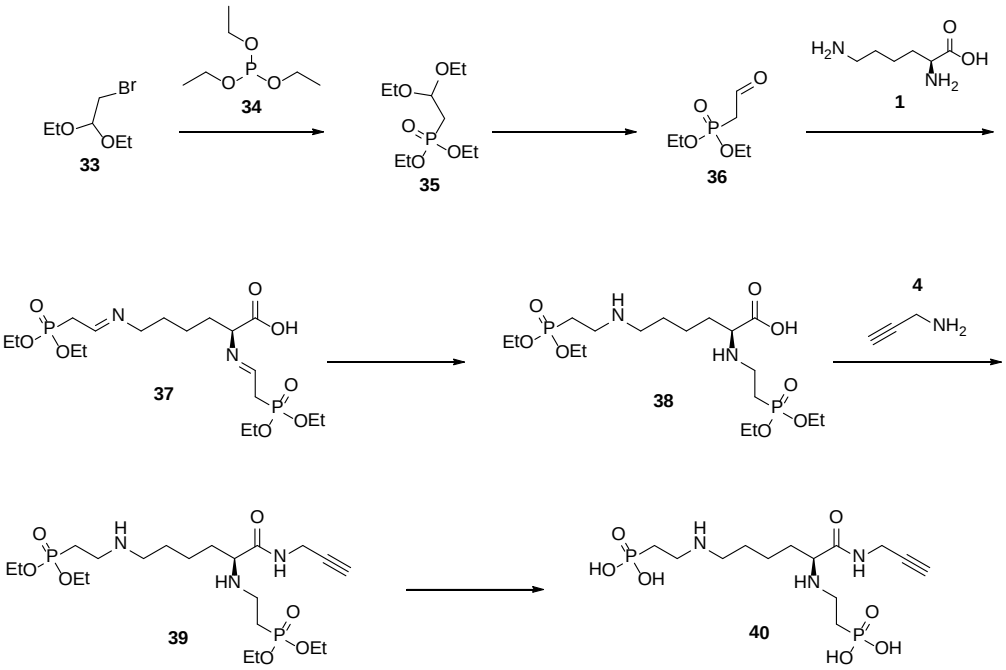

Scheme 14. Proposed synthetic pathway to generation 1 dendron via reductive amination

Starting from bromoacetaldehyde diethyl acetal **33**, this compound is reacted with triethylphosphite **34** via a Michaelis-Arbuzov reaction [42] to give diethoxyphosphonate **35**. The acetal in this compound is then hydrolysed [43] to give phosphonate aldehyde **36**. The aldehyde **36** and L-lysine **1** are reacted together via nucleophilic addition, followed by a dehydration to give the diimine **37** [44]. This is followed by a reduction [45] to yield diamine **38**. To this compound 2-propynyl amine **4** is coupled to give alkyne **39**. A final deprotection yields **G1** diphosphonate dendron **40**.

The reaction between diethyl acetal **33** and triethylphosphite **34** proceeded well and gave diethyl-(2,2-diethoxyethyl)-phosphonate **35** at 98% yield. The following deprotection of the acetal gave diethyl(2-oxoethyl)phosphonate **36** at 78% yield. The experimental procedure and ^{1}H NMR quantification of the reaction products can be found in the Supporting Information.

In an attempt to yield the L-lysine diphosphonate diimine **37**, freshly synthesised phosphonate aldehyde **36** was reacted with L-lysine in a reductive amination, with MeOH as solvent and magnesium sulphate ($MgSO_4$) as drying agent. As the formation of an imine is in equilibrium with the hydrolysis of the same group, a drying agent is needed to remove water from the reaction and drive the reaction towards the imine formation. The reaction is depicted in Scheme 15.

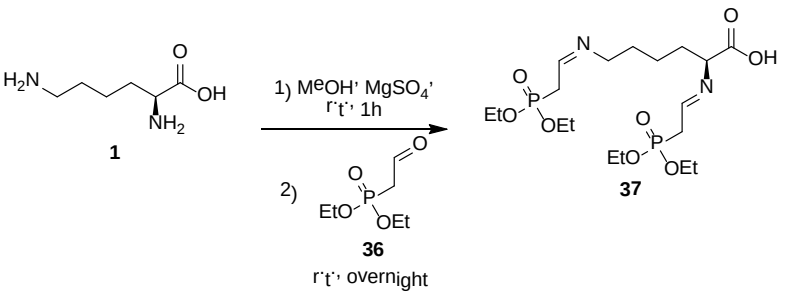

Scheme 15. Reaction with L-lysine and diethyl(2-oxoethyl)phosphonate with $MgSO_4$ as drying agent

A sample from the crude reaction mixture was analysed by MS. The resulting MS spectrum is shown in Figure 16.

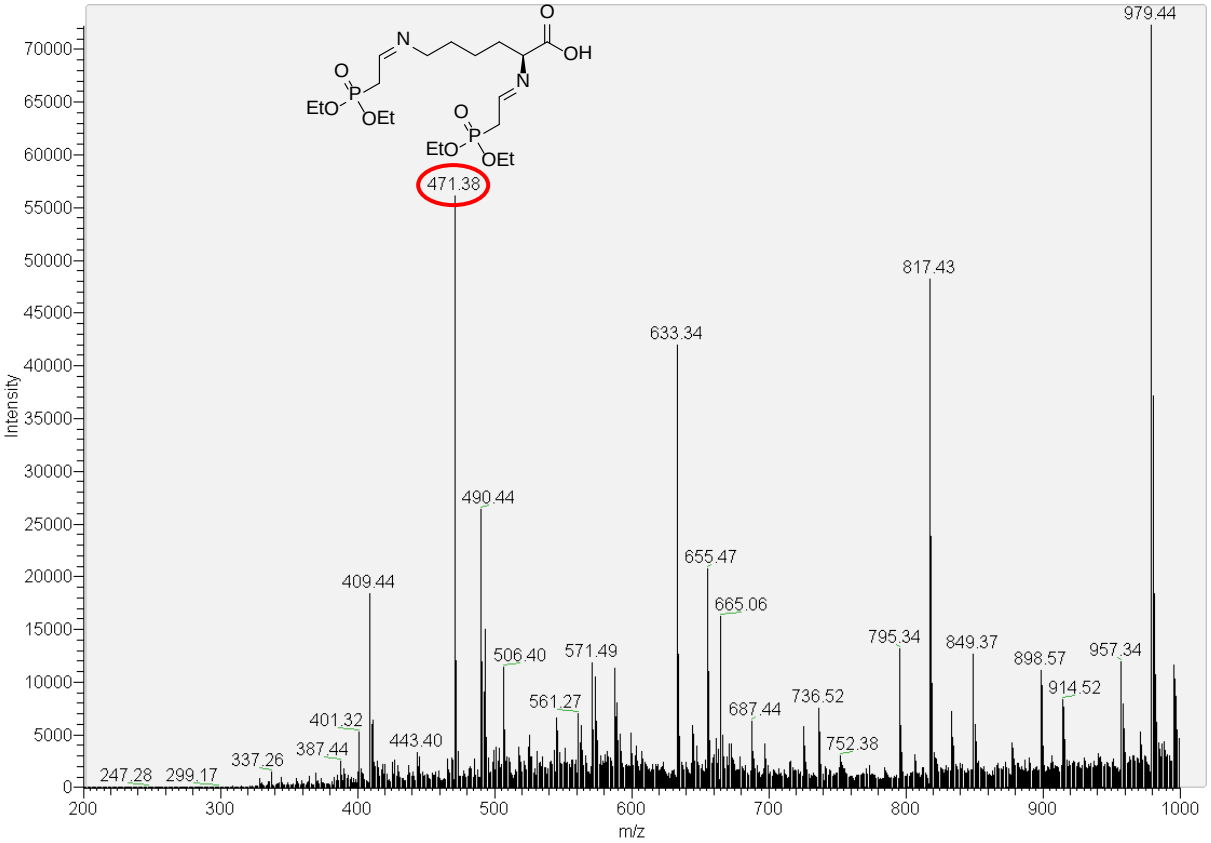

Figure 16. MS spectrum of the reductive amination using $MgSO_4$ as drying agent. The marked peak at m/z = 471.38 corresponds to the $[M+H]^+$ adduct ion of the depicted compound.

However, because of the abundance of non-product peaks, the reaction was repeated, using phosphorus pentoxide supported on silica (P_2O_5 on SiO_5) [46, 47] as drying agent and in solvent-free conditions using a mortar and pestle [48, 49]. Solvent-free conditions were chosen, because these reactions generally are easy to perform, easy to purify and the use of solvent-free conditions to create imine compounds has been researched extensively [45, 49, 50, 51]. The reaction is depicted in Scheme 16.

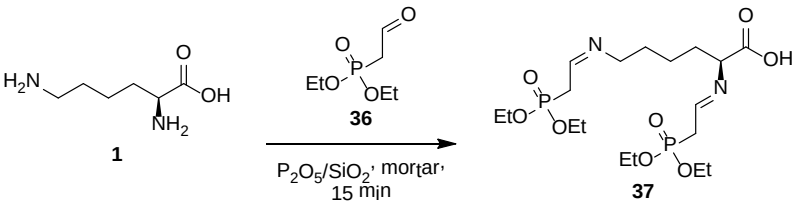

Scheme 16. Reaction with L-lysine and diethyl(2-oxoethyl)phosphonate with P_2O_5/SiO_2 as drying agent

As before, a sample of the crude reaction mixture was analysed by MS and ^{1}H NMR. The resulting MS spectrum is shown in Figure 17 and the ^{1}H NMR spectrum can be found in Figure 24 in the Supporting Information.

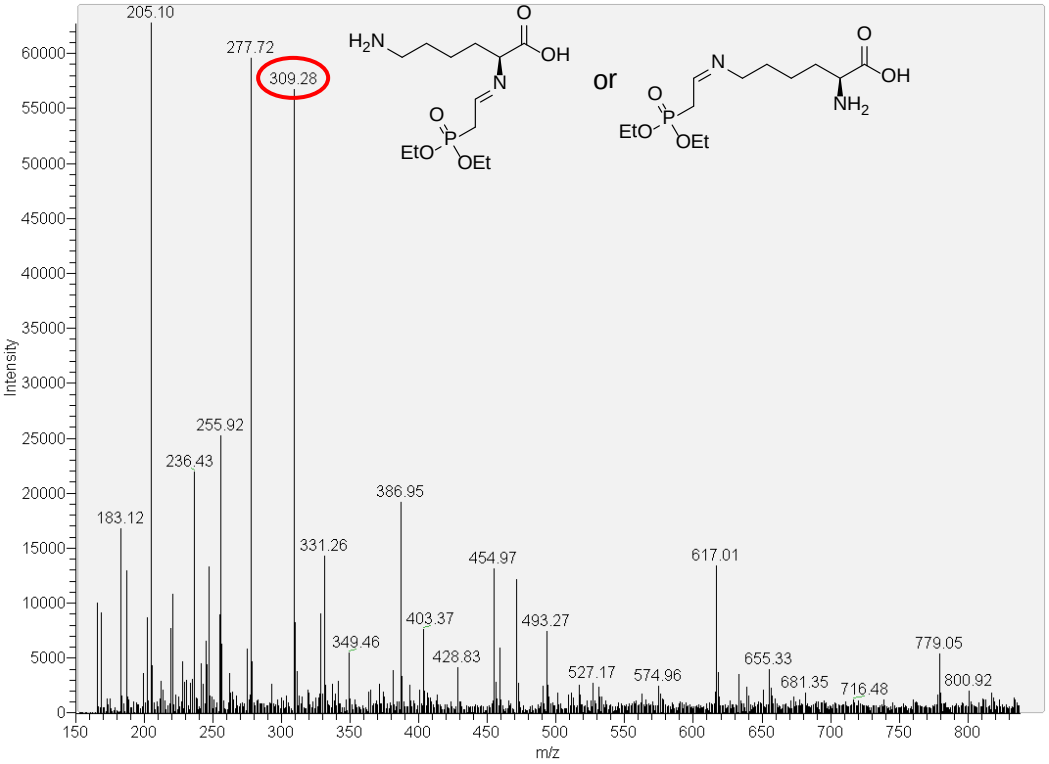

Figure 17. MS spectrum of the diimine formation using P_2O_5/SiO_2 as drying agent. The marked peak at m/z = 309.28 corresponds to the $[M+H]^+$ adduct ion of the depicted compounds.

While the analysis of the MS results shows that the reaction is proceeding, as the presence of a mono-imine product can be seen, the absence of the diimine **37** indicates that the conversion rate of the reaction is not very high. The ^{1}H NMR spectrum shows a peak that corresponds to the signal of the imine bond. However, the low integral of the peak seems to confirm the information obtained from the MS spectrum: that only mono-imines were formed. This can be caused by the fact that two of the materials used were solids and therefore did not mix optimally in a mortar, by the short reaction time (15 minutes) or a combination of both.

In an effort to increase the efficiency of the reaction, the reductive amination was repeated, using a minimal amount of MeOH to solvate the soluble compounds and increasing the reaction time to 4 days. After 2 hours, a sample of the reaction mixture was taken for MS analysis. Figure 18 shows the obtained MS spectrum.

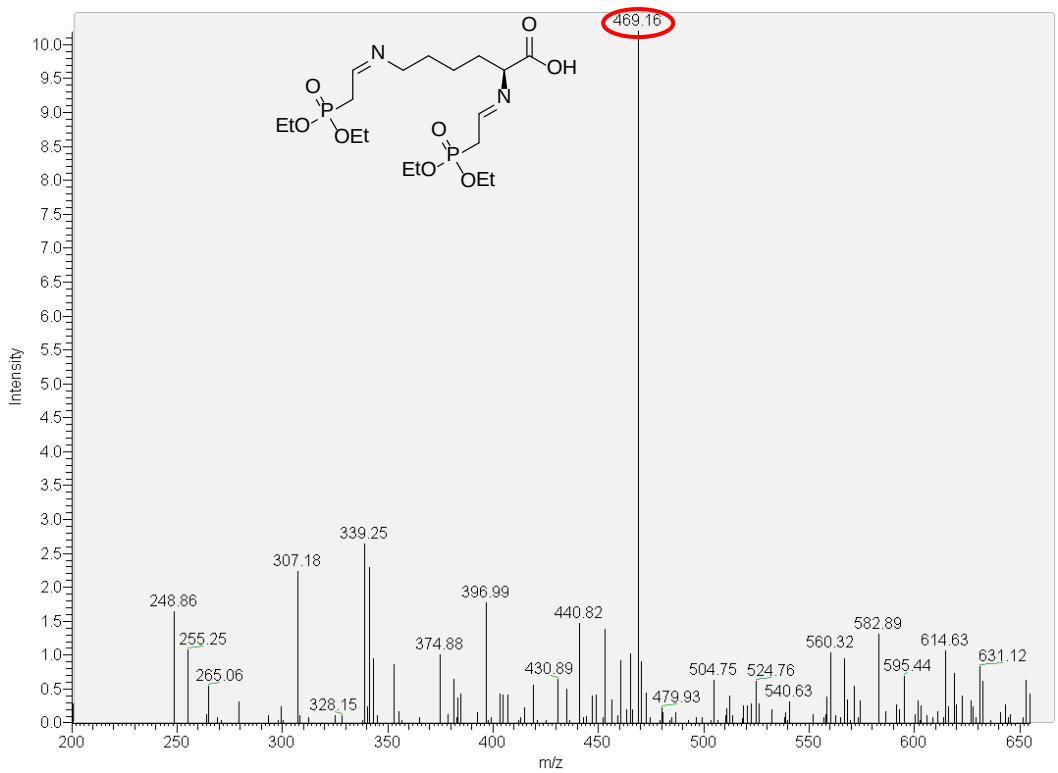

Figure 18. MS spectrum of the diimine formation using P_2O_5/SiO_2 as drying agent in MeOH. The marked peak at m/z = 469.16 corresponds to the $[M-H]^-$ adduct ion of the depicted compound.

The MS data shows that the desired diimine **37** had indeed formed after 2 hours. Therefore, it was decided to continue with the reduction of the formed diimine **37** to diamine **38** using sodium borohydride ($NaBH_4$). The reaction is shown in Scheme 17.

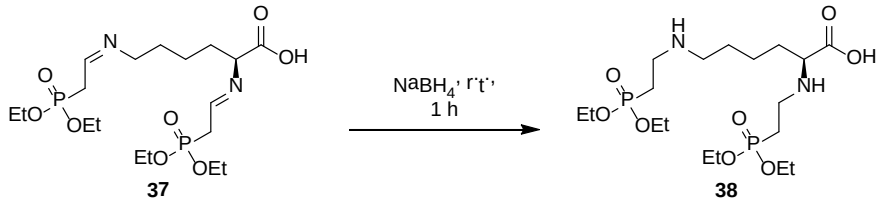

Scheme 17. Reductive amination of the diimine with $NaBH_4$

However, after an extraction was attempted to isolate the desired diamine **38** from the other compounds, ^{1}H NMR and MS analysis showed no indications to suggest that the desired compound was present. The ^{1}H NMR and MS spectra can be found in Figure 19 and Figure 20 respectively.

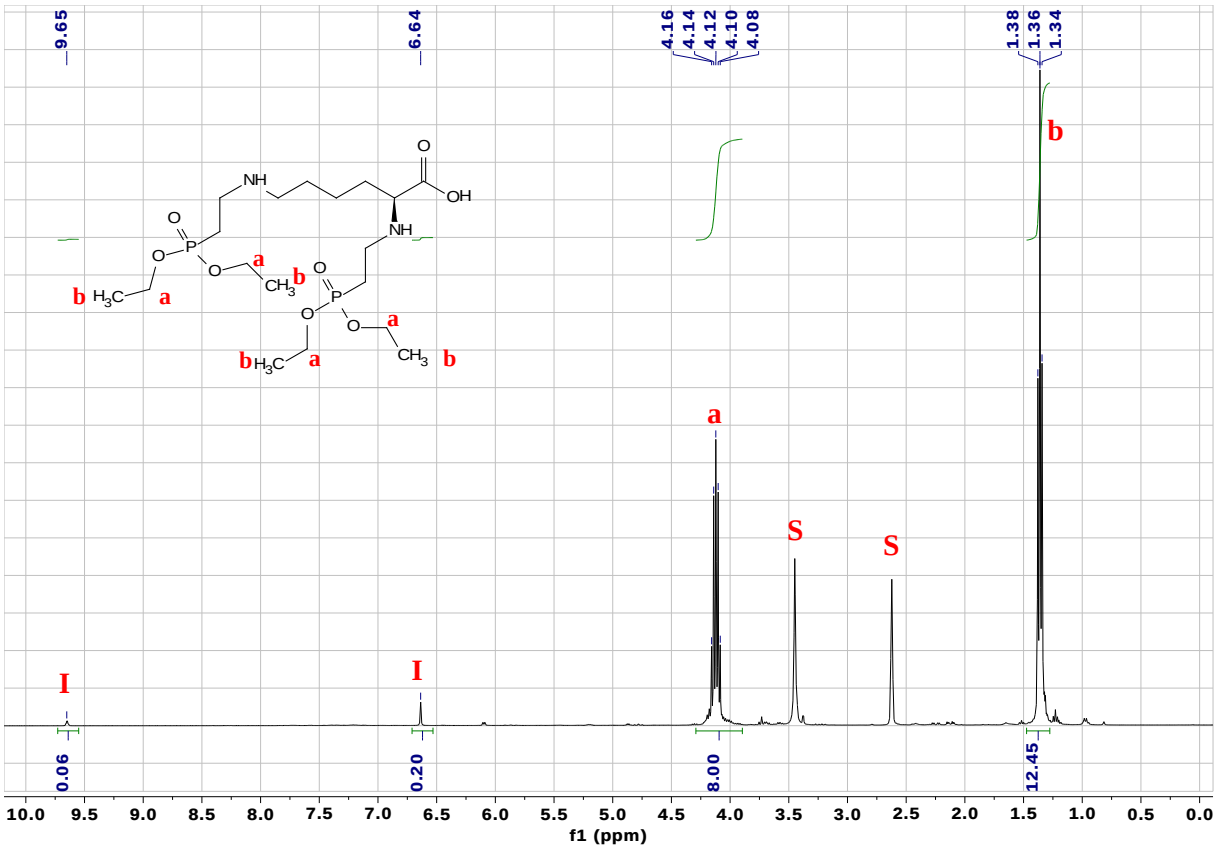

Figure 19. ^{1}**H NMR spectrum of the reductive amination after extraction. Peaks are marked as follows: impurities (I) and solvents (S).**

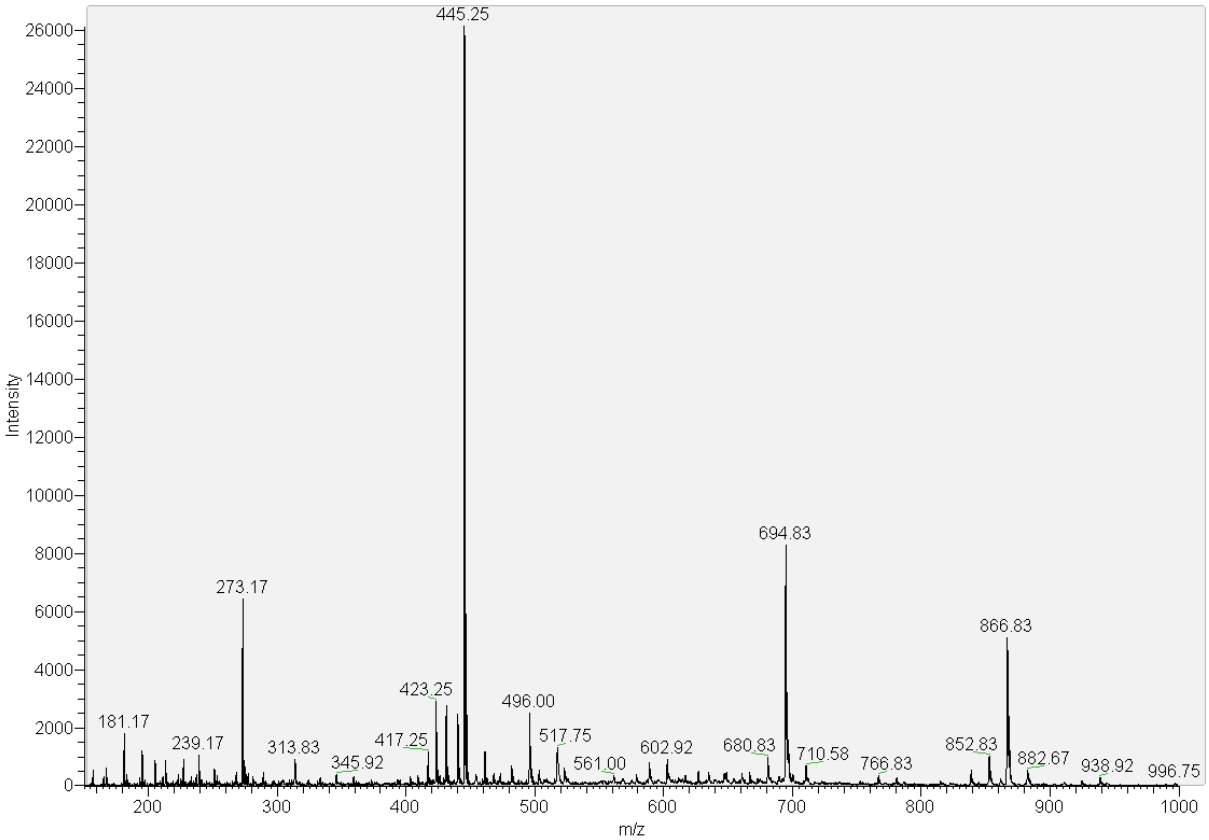

Figure 20. MS spectrum of the reductive amination after extraction

While the ^{1}H NMR spectrum shows some peaks that could be attributed to the diamine **38** (**a-b**), all the protons of the L-lysine backbone and the rest of the protons from the phosphonate tails are missing. This is supported by the MS spectrum, where none of the peaks can be attributed to adduct ions of the diamine.

It is possible that the amount of $NaBH_4$ added was not enough to facilitate the reduction, probably coupled to the presence of water in the mixture, which would quench the $NaBH_4$. Another option is that the extraction of the reaction mixture did not work as intended or that the diimine degraded over time before the reduction was attempted. However, further reaction and extraction conditions were not experimented with.

Conclusions

In this report, synthetic routes towards L-lysine-derived phosphonate-functionalised PAMAM were investigated. These routes include: 1) using CDI-mediated amide coupling with malonate and 2) the introduction of the phosphonate functionality by using reductive amination in order to produce a **G1** dendron; 3) the aza-Michael addition followed by CDI-mediated amide coupling to introduce the clickable 'head' for coupling of the second dendron, which results in a 'fast' route to produce a **G2** dendron.

While the CDI-mediated amide coupling pathway, which was proposed first, was abandoned because of a lack of success, all indications point to the wrong choice concerning starting material and/or reaction conditions as a cause for this. The proposed pathway therefore remains a possibility for further research.

Selective Michael additions, in an effort to create a **G1** dendron, proved to be impossible when performed on L-lysine, even when reaction conditions were used from literature reported to give a selective reaction. Other investigated reaction conditions also did not facilitate a selective reaction. It is speculated that this is caused by the specific chemical structure of L-lysine, with the carboxylic acid group next to one of the amine groups, which might thereby influence the reactivity of this amine when compared to the terminal amine group and thereby prevent a selective reaction

However, the attempts to create a selective Michael addition procedure led to the proposition of another pathway where the non-selective Michael addition can be used to produce a **G2** dendron. Although it was discovered that purification of this reaction was very difficult, analysis of the reaction indicated that it was actually possible to continue the pathway with this crude mixture, creating the possibility of a purification step further on.

In an effort to again find a selective way to create a L-lysine **G1** dendron, first indications prove that a reductive amination strategy might be successful in doing so. However, more research is still needed for the optimisation of the conditions and extraction procedure of this reaction.

When combined, this information creates a strong base for further studies to start their research into the production of these PAMAM dendrons.

Future work

The first route that can be further investigated is the CDI-mediated amide coupling using malonate or a related compound. Although the reaction was not successful in this study, this can be attributed to the use of malonate salt instead of the free acid of malonate. Therefore, using the free acid or a solution of the salt might result in a successful reaction and a second chance for the synthetic route described in Scheme 3.

A second option for further study is the CDI-mediated amide coupling to introduce the allyl or other 'click' functionality to the dendron and its subsequent steps described in Scheme 11. In this study, evidence was obtained suggesting that this reaction is possible. However, the product could not be isolated and further characterized. The conversion of the reaction was also very low, indicating that the reaction conditions need optimisation.

A third option is the production of a **G2** phosphonate-functionalised L-lysine dendron using the reductive amination route proposed in Scheme 14. Although evidence was obtained that suggests that the reductive amination can be performed by the method described in this report, like in the **G2** dendron experiment, no product was isolated and characterised due to lack of time. Again, optimisation of the reaction conditions and extraction procedure require can be a point for further investigation.

Although not investigated in this study, other chemical reactions could be used in the production of a L-lysine PAMAM dendron with phosphonate functionality. One of these reactions is the Moedritzer-Irani reaction (Scheme 18), which uses phosphorous acid, formaldehyde and an amine to produce a biphosphonic acid directly coupled to the nitrogen atom of the amine [52, 53]. This reaction might be an fast and easy way to give the L-lysine-based dendrons their phosphonate functionality.

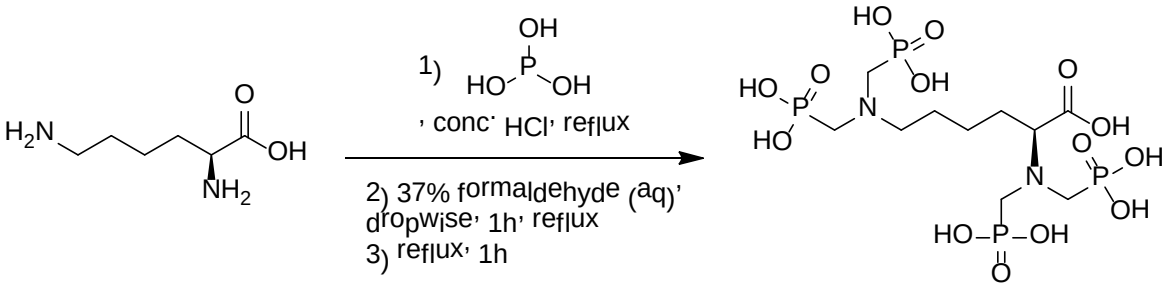

Scheme 18. Possible reaction of L-lysine using the Moedritzer-Irani reaction

Also, when the synthesis of a phosphonate dendron is successful, a second dendron is needed in order to form a complete 'Janus' dendrimer. These dendrons can readily be coupled by using an azide-alkyne Huisgen cycloaddition, using the alkyne group of the finished phosphonate dendron. A proposed synthetic route for a second dendron based on polyethylene glycol is shown in Scheme 19.

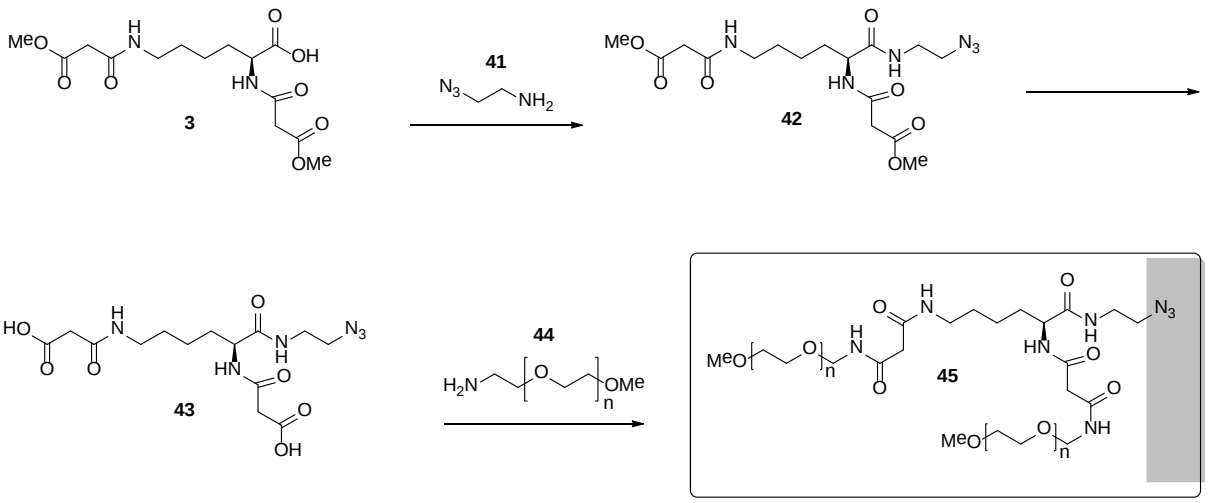

Scheme 19. Proposed synthetic route for a second dendron of the 'Janus' dendrimer, based on the coupling reaction with malonate

In this synthesis, diamide **3** is reacted with 2-azidoethanamine **41** to give azide **42**. Deprotection of this azide gives diacid azide **43**, which is coupled with aminomethoxy polyethylene glycol **44** to yield the final **G1** methoxyl polyethylene azide **45**. This polyethylene dendron can then be readily coupled to a **G1** phosphonate dendron or any other generation by an copper-catalyzed azido-alkyne Huisgen cycloaddition.

References

1. Olefjord, I.; Elfstrom, B.-O. The Composition of the Surface during Passivation of Stainless Steels. *Corrosion* **1982,** *38* (1), 46-52.
2. Sugimoto, K.; Sawada, Y. The role of molybdenum additions to austenitic stainless steels in the inhibition of pitting in acid chloride solutions. *Corrosion Science* **1977,** *17* (5), 425-445.
3. De Vito, E.; Marcus, P. XPS study of passive films formed on molybdenum-implanted austenitic stainless steels. *Surf. Interface Anal.* **1992,** *19* (1-12), 403-408.
4. Grimsdale, A. C.; Müllen, K. The Chemistry of Organic Nanomaterials. *Angew. Chem. Int. Ed.* **2005,** *44* (35), 5592-5629.
5. Ries Jr., H. E.; Cook, H. D. Monomolecular films of mixtures: I. Stearic acid with isostearic acid and with tri-*p*-cresyl phosphate. Comparison of components with octadecylphosphonic acid and with tri-*o*-xenyl phosphate. *Journal of Colloid Science* **1954,** *9* (6), 535-546.
6. Queffélec, C.; Petit, M.; Janvier, P.; Knight, D. A.; Bujoli, B. Surface Modification Using Phosphonic Acids and Esters. *Chemical Reviews* **2012,** *112*, 3777-3807.
7. Mutin, P. H.; Guerrero, G.; Vioux, A. Hybrid materials from organophosphorus coupling molecules. *J Mater Chem* **2005,** *15*, 3761-3768.
8. Raman, A.; Dubey, M.; Gouzman, I.; Gawalt, E. S. Formation of Self-Assembled Monolayers of Alkylphosphonic Acid on the Native Oxide Surface of SS316L. *Langmuir* **2006,** *22*, 6469-6472.
9. van Alsten, J. G. Self-Assembled Monolayers on Engineering Metals: Structure, Derivatization, and Utility. *Langmuir* **1999,** *15*, 7605-7614.
10. Guerrero, G.; Mutin, P. H.; Vioux, A. Organically modified aluminas by grafting and sol-gel processes involving phosphonate derivatives. *J Mater Chem* **2001,** *11* (12), 3161-3165.
11. Hotchkiss, P. J.; Jones, S. C.; Paniagua, S. A.; Sharma, A.; Kippelen, B.; Armstrong, N. R.; Marder, S. R. The Modification of Indium Tin Oxide with Phosphonic Acids: Mechanism of Binding, Tuning of Surface Properties, and Potential for Use in Organic Electronic Applications. *Accounts of Chemical Research* **2012,** *45* (3), 337-346.
12. Griep-Raming, N.; Karger, M.; Menzel, H. Using Benzophenone-Functionalized Phosphonic Acid To Attach Thin Polymer Films to Titanium Surfaces. *Langmuir* **2004,** *20*, 11811-11814.
13. Marcinka, S.; Fadeev, A. Y. Hydrolytic Stability of Organic Monolayers Supported on TiO_2 and ZrO_2. *Langmuir* **2004,** *20* (6), 2270-2273.
14. Mukherjee, S.; Huang, C.; Guerra, F.; Wang, K.; Oldfield, E. Thermodynamics of Bisphosphonates Binding to Human Bone: A Two-Site Model. *Journal of the American Chemical Society* **2009,** *131* (24), 8374-8475.
15. Mukherjee, S.; Song, Y.; Oldfield, E. NMR Investigations of the Static and Dynamic Structures of Bisphosphonates on Human Bone: a Molecular Model. *Journal of the American Chemical Society* **2008,** *130* (4), 1264-1273.
16. Demadis, K. D.; Papadaki, M.; Raptis, R. G.; Zhao, H. Corrugated, Sheet-Like Architectures in Layered Alkaline-Earth Metal *R,S*-Hydroxyphosphonoacetate Frameworks: Applications for Anticorrosion Protection of Metal Surfaces. *Chem Mater* **2005,** *20* (15), 4835-4846.
17. Fang, J. L.; Li, Y.; Ye, X. R.; Wang, Z. W.; Liu, Q. Passive Films and Corrosion Protection Due to Phosphonic Acid Inhibitors. *Corrosion* **1993,** *49* (4), 266-271.
18. Rajendran, S.; Apparao, B. V.; Palaniswamy, N. Corrosion inhibition by phosphonic acid-Zn^{2+} systems for mild steel in chloride medium. *Anti-Corrosion Methods and Materials* **2000,** *47* (6), 359-365.
19. Rajendran, S.; Apparao, B. V.; Palaniswamy, N.; Amalraj, A. J.; Sundaravadivelu, M. The role of phosphonates as transporters of Zn^{2+} ions in the inhibition of carbon steel in neutral solutions containing chlorides. *Anti-Corrosion Methods and Materials* **2002,** *49* (3), 205-209.
20. Amalric, J.; Mutin, P. H.; Guerrero, G.; Ponche, A.; Sotto, A.; Lavigne, J.-P. Phosphonate monolayers functionalized by silver thiolate species as antibacterial nanocoatings on titanium and stainless steel. *J Mater Chem* **2009,** *19* (1), 141-149.
21. Ma, H.; Acton, O.; Hutchins, D. O.; Cernetic, N.; Jen, A. K. Y. Multifunctional phosphonic acid self-assembled monolayers on metal oxides as dielectrics, interface modification layers and semiconductors for low-voltage high-performance organic field-effect transistors. *Physical Chemistry Chemical Physics* **2012,** *14* (41), 14110-14126.
22. Liu, D.; Xu, X.; Su, Y.; He, Z.; Xu, J.; Miao, Q. Self-Assembled Monolayers of Phosphonic Acids with Enhanced Surface Energy for High-Performance Solution-Processed N-Channel Organic Thin-Film Transistors. *Angew. Chem. Int. Ed.* **2013,** *52* (24), 6222-6227.
23. Michel, R.; Lussi, J. W.; Csucs, G.; Reviakine, I.; Danuser, G.; Ketterer, B.; Hubbell, J. A.; Textor, M.; Spencer, N. D. Selective Molecular Assembly Patterning: A New Approach to Micro- and Nanochemical Patterning of Surfaces for Biological Applications. *Langmuir* **2002,** *18*, 3281-3287.
24. Tomalia, D. A.; Baker, H.; Dewald, J.; Hall, M.; Kallos, G.; Martin, S.; Roeck, J.; Ryder, J.; Smith, P. A New Class of Polymers: Starburst-Dendritic Macromolecules. *Polymer Journal* **1985,** *17*, 117-132.
25. Maruo, N.; Uchiyama, M.; Kato, T.; Arai, T.; Akisada, H.; Nishino, N. Hemispherical synthesis of dendritic poly(**L**-Lysine) combining sixteen free-base porphyrins and sixteen zinc porphyrins. *Chemical Communications* **1999**, 2057-2058.
26. Lee, J. W.; Kim, J. H.; Kim, B.-K. Synthesis of azide-funtionalized PAMAM dendrons at the focal point and their application for synthesis of PAMAM-like dendrimers. *Tetrahedron Letters* **2006,** *47*, 2683-2686.
27. Grayson, S. M.; Fréchet, J. M. J. Convergent Dendrons and Dendrimers: from Synthesis to Applications. *Chemical Reviews* **2001,** *101*, 3819-3867.

28. Tomalia, D. A.; Naylor, A. M.; Goddard, W. A. Starburst Dendrimers: Molecular-Level Control of Size, Shape, Surface Chemistry, Topology, and Flexibility from Atoms to Macroscopic Matter. *Angew. Chem. Int. Ed. Engl.* **1990,** *29* (2), 138-175.
29. Hawker, C. J.; Fréchet, J. M. J. Preparation of polymers with controlled molecular architecture. A new convergent approach to dendritic macromolecules. *Journal of the American Chemical Society* **1990,** *112* (21), 7638-7647.
30. Caminade, A.-M.; Laurent, R.; Delavaux-Nicot, B.; Majoral, J.-P. ''Janus'' dendrimers: syntheses and properties. *New Journal of Chemistry* **2012,** *36*, 217-226.
31. Michael, A. On the addition of sodium acetacetic ether and analogous sodium compounds to unsaturated organic ethers. *American Chemistry Journal* **1887,** *9*, 115.
32. Métro, T.-X.; Bonnamour, J.; Reidon, T.; Sarpoulet, J.; Martinez, J.; Lamaty, F. Mechanosynthesis of amides in the total absence of organic solvent from reaction to product recovery. *Chemical Communications* **2012,** *48*, 11781-11783.
33. Verma, S. K.; Ghorpade, R.; Pratap, A.; Kaushik, M. P. Solvent free, *N,N'*-carbonyldiimidazole (CDI) mediated amidation. *Tetrahedron Letters* **2012,** *53* (19), 2372-2376.
34. Tanaka, K.; Toda, F. Solvent-Free Organic Synthesis. *Chemical Reviews* **2000,** *100*, 1025-1074.
35. Maliakal, A.; Katz, H.; Cotts, P. M.; Subramoney, S.; Mirau, P. Inorganic Oxide Core, Polymer Shell Nanocomposite as a High *K* Gate Dielectric for Flexible Electronics Applications. *Journal of the American Chemical Society* **2005,** *127*, 14655-14662.
36. Paul, R.; Anderson, G. W. N,N'-Carbonyldiimidazole, a New Peptide Forming Reagent. *Journal of the American Chemical Society* **1960,** *82* (17), 4596-4600.
37. Jose, J.; Burgess, K. Syntheses and Properties of Water-Soluble Nile Red Derivatives. *Journal of Organic Chemistry* **2006,** *71*, 7835-7839.
38. Ranu, B. C.; Banerjee, S. Significant rate acceleration of the aza-Michael reaction in water. *Tetrahedron Letters* **2006,** *48*, 141-143.
39. Wabnitz, T. C.; Yu, J.-Q.; Spencer, J. B. Evidence That Protons Can Be the Active Catalysts in Lewis Acid Mediated Hetero-Michael Addition Reactions. *Chemistry - A European Journal* **2004,** *10*, 484-493.
40. Chaudhuri, M. K.; Hussain, S.; Kantam, M. L.; Neelima, B. Boric acid: a novel and safe catalyst for aza-Michael reactions in water. *Tetrahedron Letters* **2005,** *46* (48), 8329-8331.
41. Lind, T. K.; Polcyn, P.; Zielinska, P.; Cárdenas, M.; Urbanczyk-Lipkowska, Z. On the Antimicrobial Activity of Various Peptide-Based Dendrimers of Similar Architecture. *Molecules* **2015,** *20*, 738-753.
42. Lukáč, M.; Garajová, M.; Mrva, M.; Devínsky, F.; Ondriska, F.; Kubincová, J. Novel fluorinated dialkylphosphonatocholines: Synthesis, physicochemical properties and antiprotozoal activities against *Acanthamoeba* spp. *Journal of Fluorine Chemistry* **2014,** *164*, 10-17.
43. Apana, S. M.; Anderson, L. W.; Berridge, M. S. Synthesis and biodistribution of [^{11}C]SN-38. *Journal of Labelled Compounds and Radiopharmaceuticals* **2010,** *53*, 178-182.
44. Jarrahpour, A. A.; Motamedifar, M.; Pakshir, K.; Hadi, N.; Zarei, M. Synthesis of Novel Azo Schiff Bases and Their Antibacterial and Antifungal Activities. *Molecules* **2004,** *9*, 815-824.
45. Cho, B. T.; Kang, S. K. Direct and indirect reductive amination of aldehydes and ketones with solid acid-activated sodium borohydride under solvent-free conditions. *Tetrahedron* **2005,** *61*, 5725-5734.
46. Eshghi, H.; Hassankhani, A. Phosphorus pentoxide supported on silica gel and alumina (P_2O_5/SiO_2, P_2O_5/Al_2O_3) as useful catalysts in organic synthesis. *Journal of the Iranian Chemical Society* **2012,** *9*, 467-482.
47. Siddiqui, Z. N.; Khan, T. P_2O_5/SiO_2 as an efficient heterogeneous catalyst for the synthesis of heterocyclic alkene derivatives under thermal solvent-free conditions. *Catalysis Science & Technology* **2013,** *3*, 2032-2043.
48. Devidas, S. M.; Quadri, S. H.; Kamble, S. A.; Syed, F. M.; Vyavhare, D. Y. Novel One-Pot Synthesis of Schiff Base Compounds Derived From Different Diamine & Aromatic Aldehyde Catalyzed by P_2O_5/SiO_2 Under Free-Solvent Condition at Room Temperature. *Journal of Chemical and Pharmaceutical Research* **2011,** *3* (2), 489-495.
49. Naeimi, H.; Sharghi, H.; Salimi, F.; Rabiei, K. Facile and Efficient Method for Preparation of Schiff Base Catalyzed By P_2O_5/SiO_2 under Free Solvent Conditions. *Heteroatom Chemistry* **2008,** *19* (1), 43-47.
50. Kaitner, B.; Zbačnik, M. Solvent-free Mechanosynthesis of Two Thermochromic Schiff Bases. *Acta Chimica Slovenica* **2012,** *59*, 670-679.
51. Zarei, M.; Jarrahpour, A. Green and efficient synthesis of azo Schiff bases. *Iranian Journal of Science & Technology* **2011,** *A3*, 235-242.
52. Moedritzer, K.; Irani, R. R. The Direct Synthesis of α-Aminomethylphosphonic Acids. Mannich-Type Reactions with Orthophosphorous Acid. *Journal of Organic Chemistry* **1965,** *31*, 1603-1607.
53. Redmore, D. Chemistry of Phosphorous Acid: New Routes to Phosphonic Acids and Phosphate Esters. *Journal of Organic Chemistry* **1978,** *43* (5), 992-996.

Supporting Information

Solvents and reagents were used as supplied by Sigma-Aldrich and Acros Organics. Silica column chromatography was carried out using silica gel provided by Silicycle Inc. (40-63 µm), alumina column chromatography was carried out using aluminium oxide powder provided by Merck (Aluminium oxide 60 GF_{254} neutral (Type E)) and reversed phase chromatography was carried out using silica gel provided by Fluka (Silica gel 100 C_{18}-Reversed phase). Thin-layer chromatography was performed on commercially available Merck aluminium backed silica gel 60 F_{254} plates, Merck glass backed C_{18}-silica gel 60 RP-18 F_{254}s plates and Merck aluminium backed aluminium oxide 60 F_{254} neutral Type E plates. Proton ^{1}H NMR spectra were recorded on a Brucker Ultrashield™ 400 (^{1}H 400 MHz) at 25 °C. Chemical shifts (δ) are quoted in parts per million, referenced to residual solvent. Positive and negative ion electrospray mass spectra were recorded on a Finnigan LXQ mass spectrometer.

Experimental section

(S)-2,6-bis(3-methoxy-3-oxopropanamido)hexanoic acid (3)

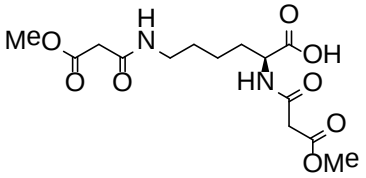

To 1.08 g of methyl potassium malonate (6.92 mmol) in a mortar was added 1.12 g of carbonyldiimidazole (6.91 mmol) and the mixture was grinded for 15 minutes. L-lysine monohydrate (0.570 g, 3.47 mmol) was added and the mixture was again grinded for 15 minutes. Water was added and the solution was analysed by MS.

Methyl potassium malonate (0.951 g, 6.09 mmol) was suspended in 150 ml of ethyl acetate (EtOAc) and the solution was placed under N_2 atmosphere. To the suspension was added 0.856 ml of Et_3N (6.09 mmol) and the mixture was stirred for 5 minutes before the temperature was brought to 0 °C with an ice bath. HOBt (0.823 g, 6.09 mmol) and DCC (1.26 g, 6.11 mmol) were added, the ice bath was removed and the mixture was stirred for 30 minutes. L-lysine monohydrate (0.502 g, 3.06 mmol) was added and the reaction was left to stir overnight at room temperature. The mixture was filtered and the filtrate was washed with 100 ml 1M HCl and 3x 50 ml water. The organic layer was dried over $MgSO_4$ and evaporated under reduced pressure. The residue was analysed by ^{1}H NMR.

L-lysine methyl ester diacid (18)

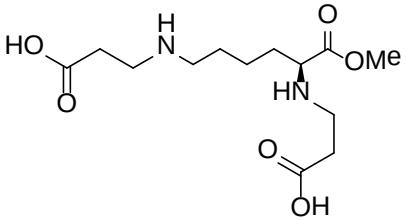

L-lysine methyl ester (3.03 g, 13.0 mmol) and acrylic acid (2.65 ml, 38.6 mmol) were added to 5 ml of water, heated to 70 °C and stirred for 4 days. The resulting mixture was analysed by MS.

(S)-2,6-bis((3-methoxy-3-oxopropyl)amino)hexanoic acid (23)

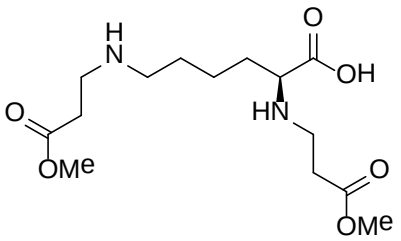

L-lysine monohydrate (0.705 g, 4.29 mmol) was dissolved in 10 ml water. To the solution was added methyl acrylate (1.20 ml, 13.3 mmol) and the mixture was stirred for 30 minutes at room temperature. The resulting mixture was analysed by MS.

L-lysine monohydrate (0.504 g, 3.07 mmol) was dissolved in 10 ml water and the solution was cooled to 0 °C with an ice bath. To the solution was added methyl acrylate (0.820 ml, 9.11 mmol) and the mixture was stirred for 40 minutes at 0 °C. The resulting mixture was analysed by MS.

(S)-2,6-bis((3-(tert-butoxy)-3-oxopropyl)amino)hexanoic acid (25)

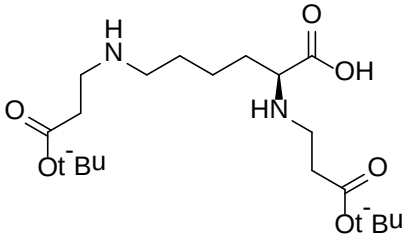

L-lysine monohydrate (0.493 g, 3.00 mmol) was dissolved in 10 ml water and the solution was cooled to 0 °C with an ice bath. To the solution was added tert-butyl acrylate (1.40 ml, 9.56 mmol) and the mixture was stirred for 30 minutes at 0 °C. The resulting mixture was analysed by MS.

L-lysine monohydrate (1.02 g, 6.21 mmol) was dissolved in 20 ml water and the solution was cooled to 0 °C with an ice bath. To the solution was added tert-butyl acrylate (1.80 ml, 12.3 mmol) and the mixture was stirred for 5 hours at 0 °C. The mixture was analysed by MS every 20 minutes.

L-lysine methyl ester ditert-butyl ester (26)

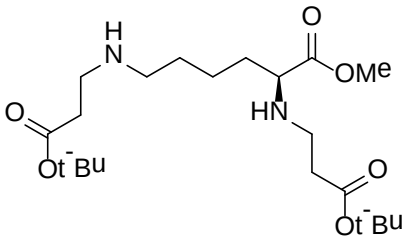

L-lysine methyl ester (0.506 g, 2.17 mmol) was dissolved in 10 ml water and the solution was cooled to 0 °C with an ice bath. To the solution was added tert-butyl acrylate (0.980 ml, 6.69 mmol) and the mixture was stirred overnight (17 hours) initially at 0 °C and later at room temperature. The resulting mixture was analysed by MS.

(S)-2,6-bis(bis(3-methoxy-3-oxopropyl)amino)hexanoic acid (27)

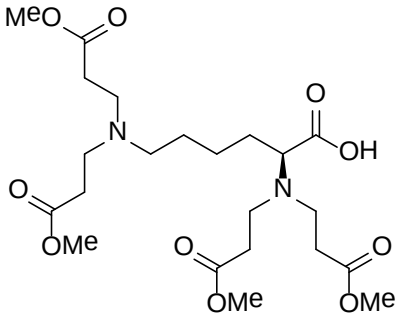

L-lysine monohydrate (1.01 g, 6.15 mmol) was suspended in 15 ml of MeOH. To this suspension were added 0.250 g of NaOH (6.25 mmol) and 3.30 ml of methyl acrylate (36.6 mmol). The mixture was stirred at reflux for 7 days, then cooled. The solvent was evaporated under reduced pressure. The residue was shaken with 6.20 ml of ice-cold 1M HCl in MeOH and 30 ml of acetone. The resulting suspension was filtered and the filtrate was evaporated under reduced pressure. The residue was purified by reversed phase column chromatography, which was eluted with water/acetonitrile (3:1) to give a sticky yellow-brown oil that contained both the tri- and the tetra-adduct. MS $[M+H]^+$: found 491.40; calculated 491.2605.

Tetra-adduct vinyl amide (30)

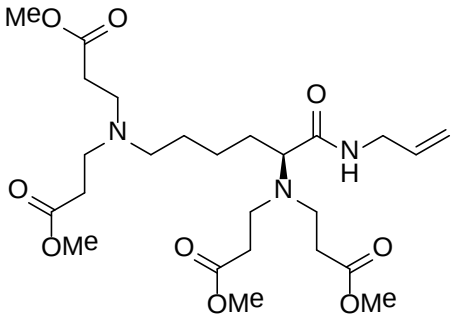

To 1.12 g of the tri- and tetra-adduct mixture **27** (2.28-2.77 mmol) in a mortar was added carbonyldiimidazole (0.580 g, 3.58 mmol) and the mixture was grinded until the evolution of CO_2 had stopped. An additional amount of carbonyldiimidazole was added, until all of the solid starting material had turned into an oil and CO_2 evolution had stopped. To this oil was then added allyl amine (0.415 ml, 5.54 mmol) and the mixture was left to react for 2 hours with occasional grinding. MeOH was added to the mixture and the crude solution was analysed by MS.

Diethyl (2,2-diethoxyethyl)phosphonate (35)

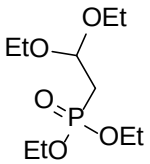

Triethylphosphite (4.56 ml, 26.6 mmol) was mixed with 2-bromo-1,1-diethoxyethane (2.00 ml, 13.3 mmol), heated at 180 °C and stirred for 4 hours. The reaction mixture was cooled and purified by flash chromatography with EtOAc as eluent to yield the product (98%).

^{1}H NMR (400 MHz, $CDCl_3$): δ = 5.030 (dt, J = 5.2 Hz & J = 5.6 Hz, 1H), 4.237 (quint, J = 7.4 Hz, 4H), 3.733 (dquint, J = 43.2 Hz & J = 7.2 Hz & J = 8.4 Hz, 4H), 2.329 (dd, J = 5.6 Hz & J = 18.4 Hz, 2H), 1.494-1.434 (m, 6H), 1.385-1.321 (m, 6H). MS $[M+Na]^+$: found 277.1171; calculated 277.1181.

Diethyl (2-oxoethyl)phosphonate (36)

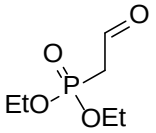

To diethyl (2,2-diethoxyethyl)phosphonate (3.20 g, 12.5 mmol) was added 20 ml of 1M HCl. The suspension was saturated with N_2 during 30 min. The reaction was then stirred at reflux for 1 hour under N_2. The mixture was cooled and saturated with NaCl. The water layer was subsequently extracted with CH_2Cl_2 (5x 20 ml) and the organic layer evaporated under reduced pressure to yield the product (76%).

^{1}H NMR (400 MHz, $CDCl_3$): δ = 9.661 (dt, J = 0.8 Hz & J = 3.2 Hz, 1H), 4.189-4.079 (m, 4H), 3.079 (dd, J = 3.2 Hz & J = 22 Hz, 2H), 1.361-1.298 (m, 6H). MS $[M+Na+CH_3OH]^+$: found 235.0707; calculated 235.0711.

(S)-2-((E)-(2-(diethoxyphosphoryl)ethylidene)amino)-6-((Z)-(2-(diethoxyphosphoryl)ethylidene)amino)hexanoic acid (37)

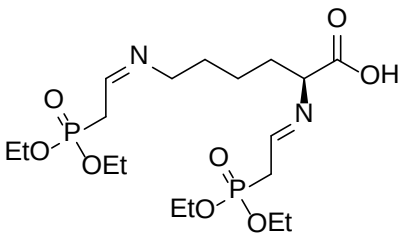

L-lysine monohydrate (0.384 g, 2.34 mmol) was dissolved in 50 ml MeOH. To this solution was added about 5.60 g of $MgSO_4$ and the suspension was stirred for 1 hour. Diethyl (2-oxoethyl)phosphonate **36** (1.04 g, 5.77 mmol) was added and the mixture was left to stir overnight. The resulting mixture was analysed by MS.

L-lysine monohydrate (69.0 mg, 0.420 mmol) dissolved in 5 ml MeOH. To this solution was added about 100 mg of P_2O_5/SiO_2 and the suspension was stirred for 5 minutes. Diethyl (2-oxoethyl)phosphonate **36** (0.152 g, 0.844 mmol) was added and the mixture was stirred for 4 days. The mixture was analysed by MS during the first hours of the reaction.

(S)-2,6-bis((2-(diethoxyphosphoryl)ethyl)amino)hexanoic acid (38)

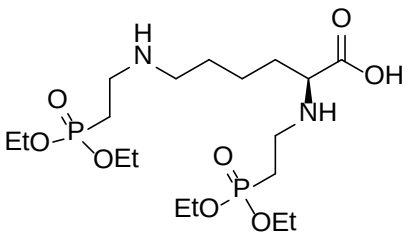

To the unpurified reaction mixture of **37** was added sodium borohydride (36.0 mg, 0.952 mmol) and the mixture was stirred until evolution of H_2 had stopped. The reaction was then stirred for 1 hour. After 1 hour, 10 ml of saturated aqueous $NaHCO_3$ was added to quench the reaction. The pH of the mixture was adjusted to ± 6 with 1M HCl and the mixture was filtered. The filtrate was extracted with 3x 30 ml EtOAc and the combined organic layers were washed with brine and dried over $MgSO_4$. The solvent was evaporated under reduced pressure and the residue was analysed by MS and ^{1}H NMR.

NMR spectra

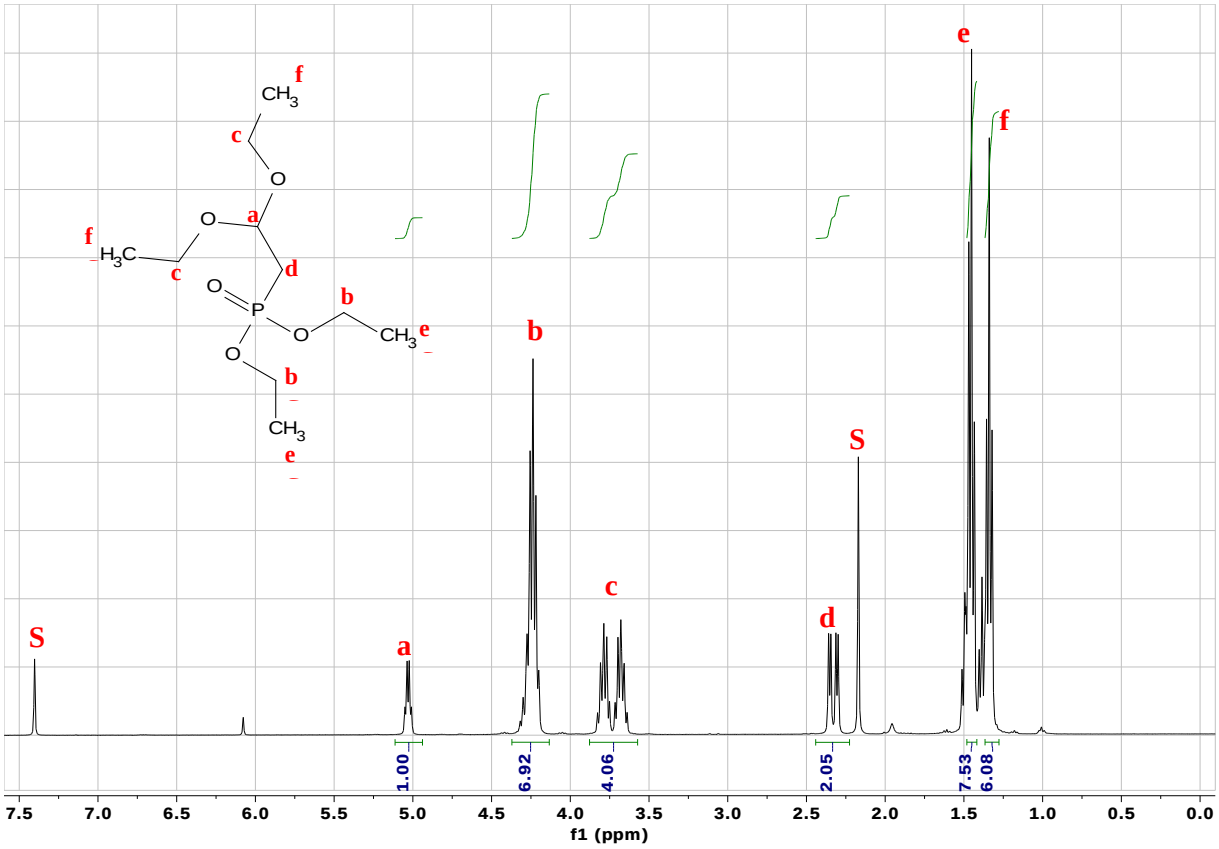

Figure 21. ^{1}H NMR spectrum of diethyl (2,2-diethoxyethyl)phosphonate. Solvent peaks are marked S. Increased integrals at peak b and e are caused by the presence of leftover triethylphosphite. Obtained in $CDCl_3$.

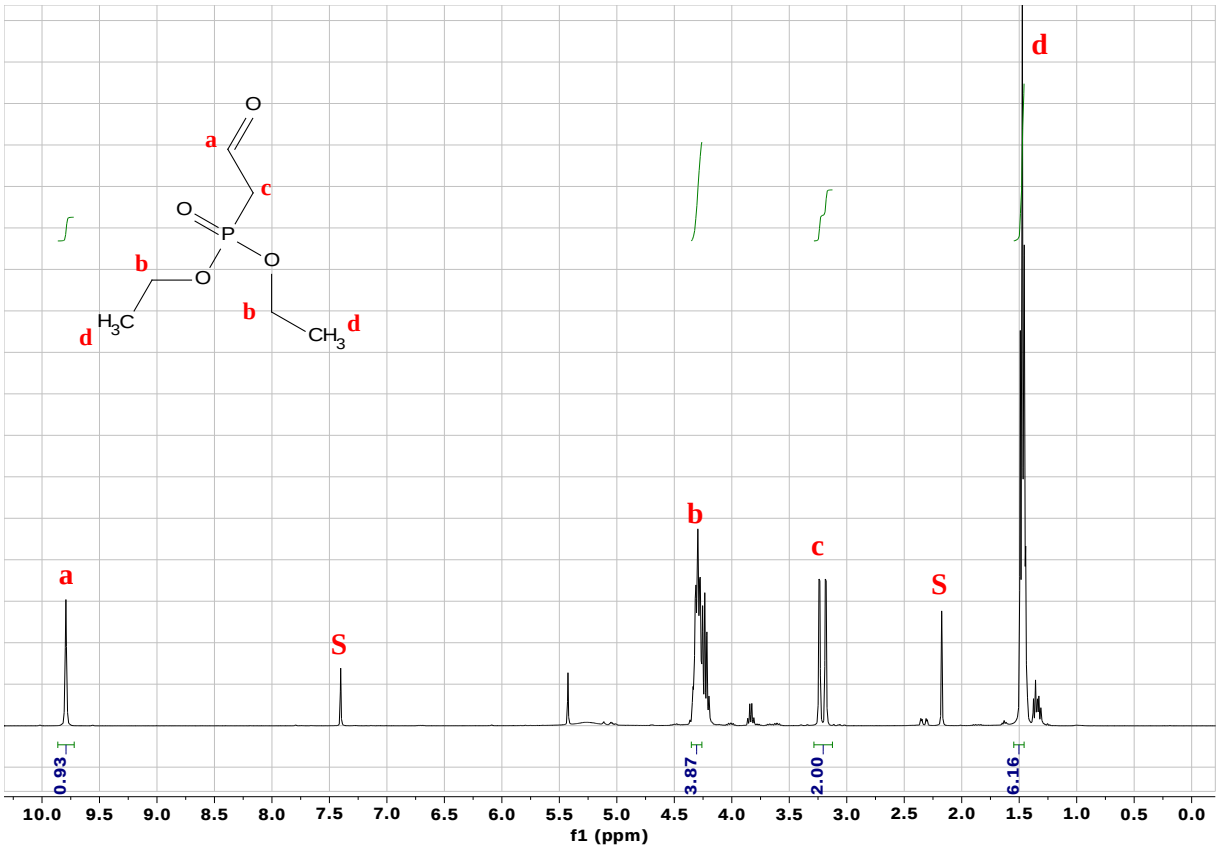

Figure 22. ^{1}H NMR spectrum of diethyl (2,2-diethoxyethyl)phosphonate. Solvent peaks are marked S. Other peaks are small impurities. Obtained in $CDCl_3$.

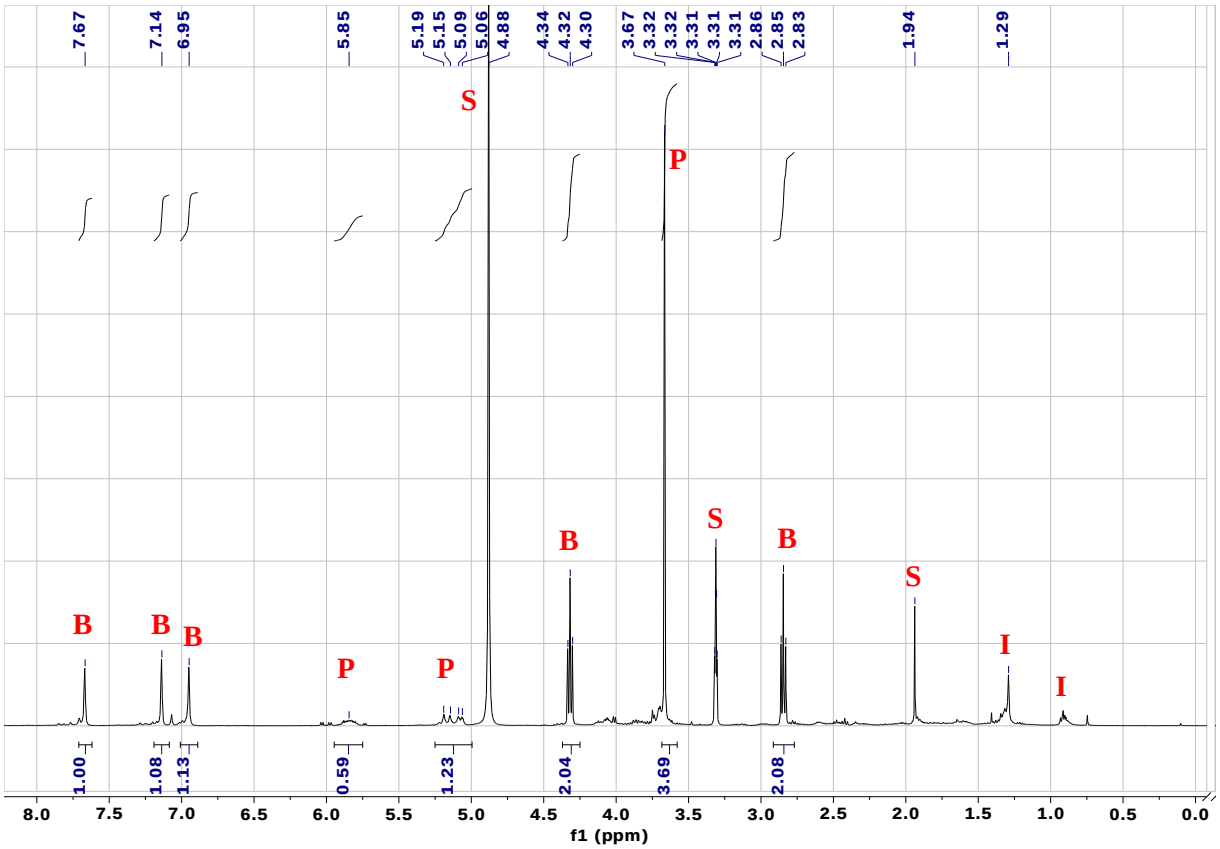

Figure 23. ^{1}H NMR spectrum of the amide coupling reaction between the tri- & tetra-adduct mixture and allyl amine after column purification. Peaks are marked as follows: solvents (S), vinyl product (P), by-product (B) and impurity (I). Obtained in CD_3OD.

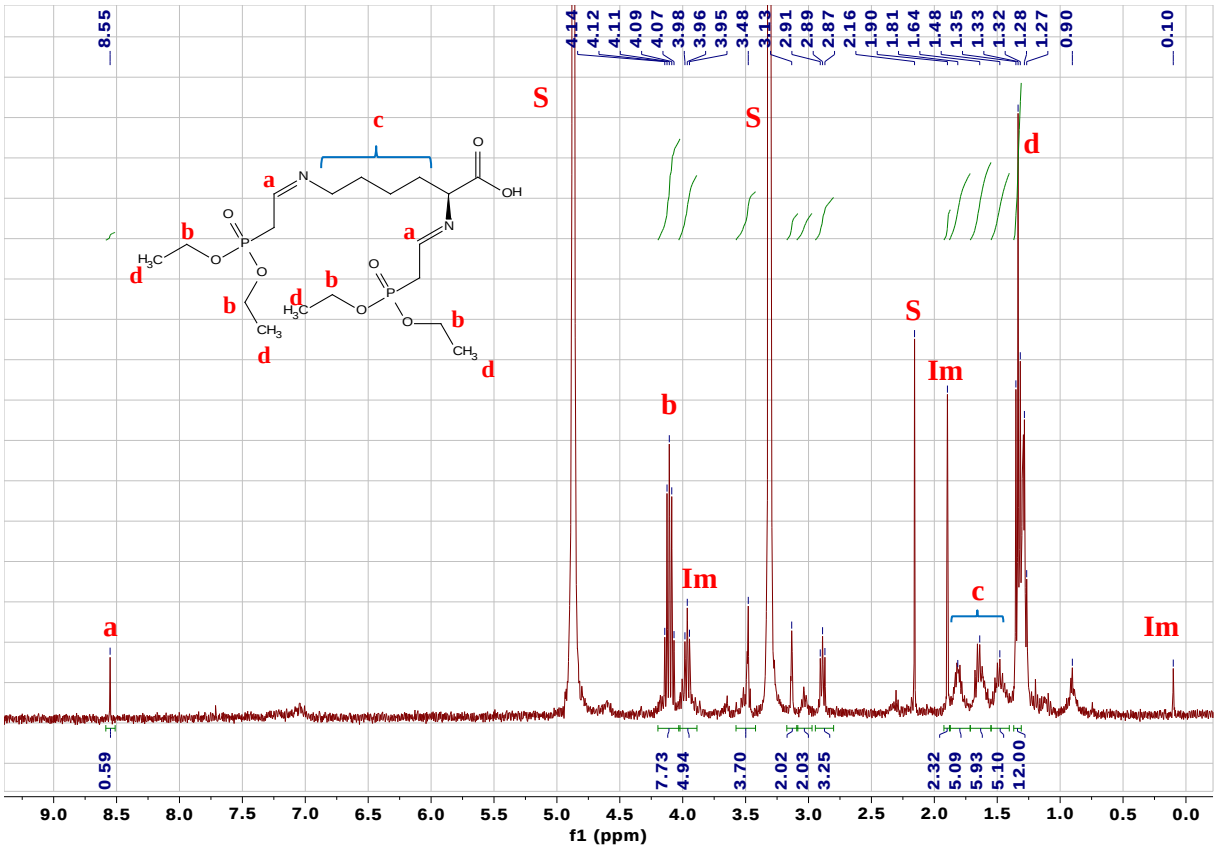

Figure 24. ^{1}H NMR spectrum of the diimine formation using P_2O_5/SiO_2 as drying agent. Peaks are marked as follows: impurities(Im), solvent peaks (S), product (a-d). The structure of the desired diimine product is shown. Obtained in MeOD.

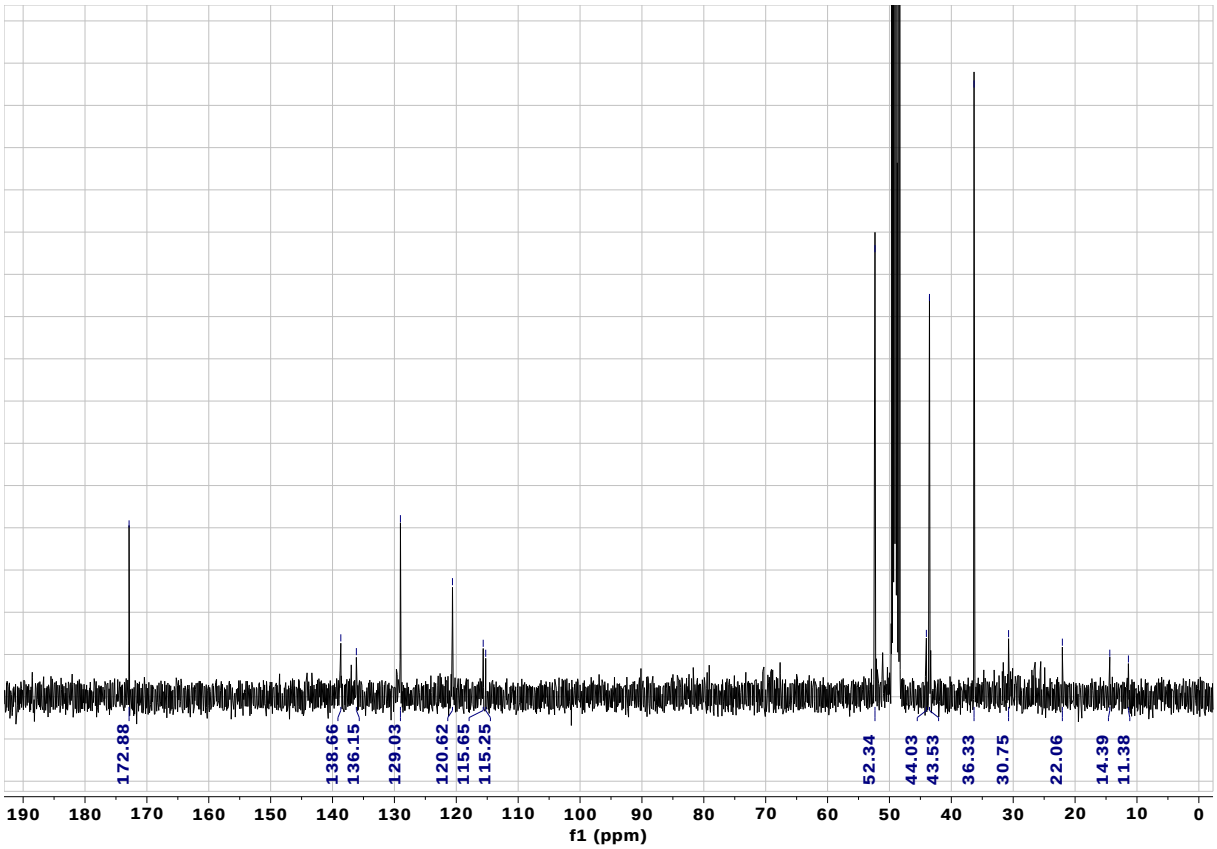

Figure 25. ^{13}C NMR of the amide coupling reaction between the tri- & tetra-adduct mixture and allyl amine after column purification. Obtained in CD_3OD.

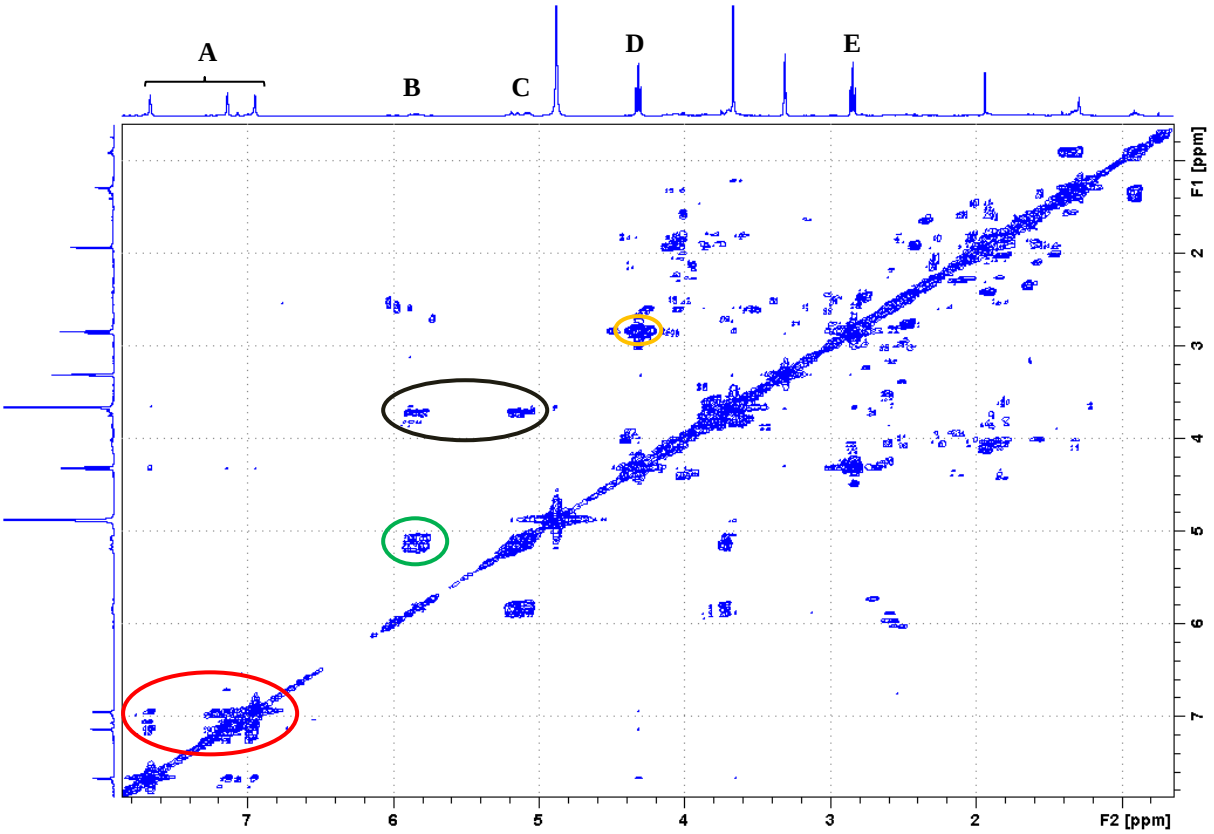

Figure 26. 2D COSY NMR spectrum of the amide coupling reaction between the tri- & tetra-adduct mixture and allyl amine after column purification. ^{1}H NMR spectra of the same sample are shown on the x- and y-axis. The marked regions represent as follows: interactions between aromatic protons A (red); interaction between vinyl protons B and C (green); interaction of vinyl protons B & C with neighbouring protons D (black); interaction of triplet D with triplet E (orange). Obtained in CD_3OD.

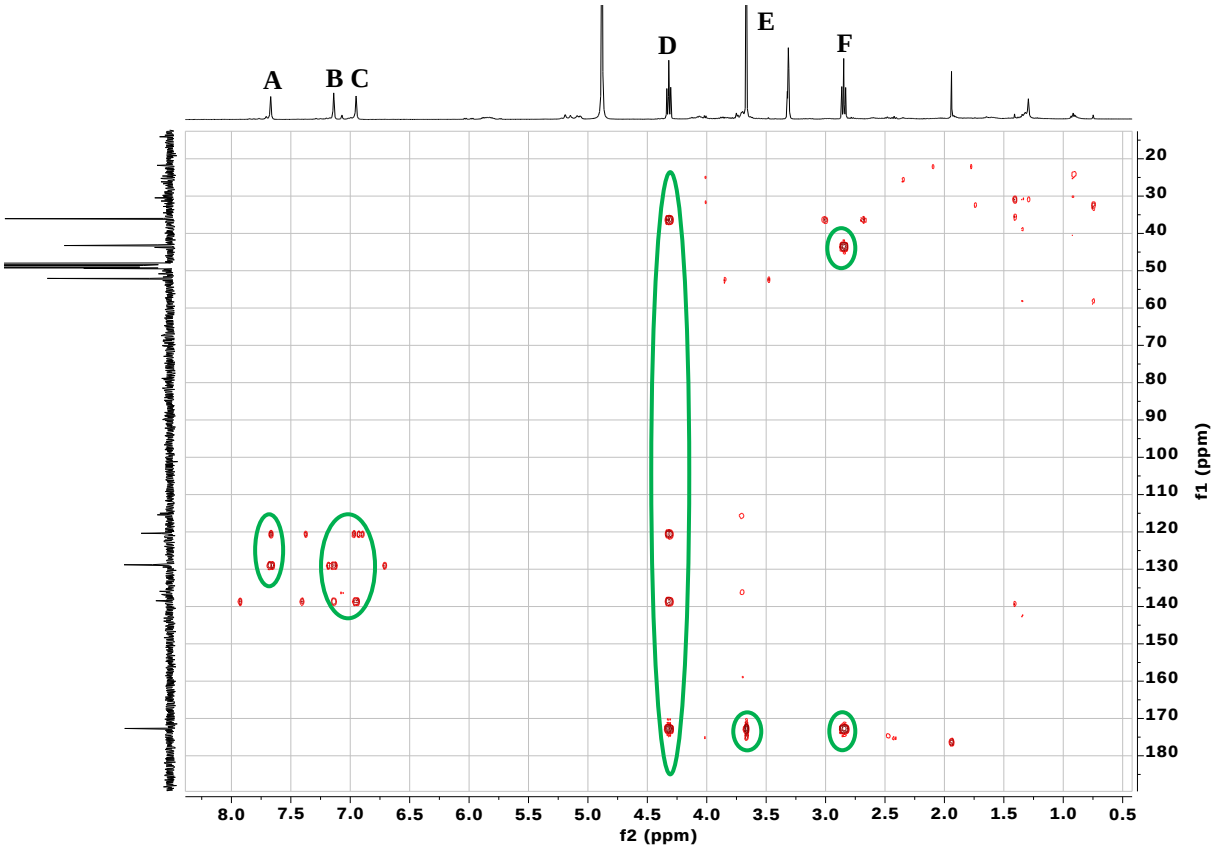

Figure 27. 2D HMBC NMR spectrum of the amide coupling reaction between the tri- & tetra-adduct mixture and allyl amine after column purification, with the ^{1}H NMR spectrum on the x-axis and the ^{13}C NMR spectrum on the y-axis. Circled signals belonging to peaks A-F are analysed below. Obtained in CD_3OD.

Table 6. Peak analysis of the 2D HMBC NMR spectrum

Peak	^{1}H NMR signal (ppm)	^{13}C NMR signals (ppm)
A	7.669	120.63, 129.04
B	7.139	129.04, 138.67
C	6.951	120.63, 138.67
D	4.319	36.33, 120.63, 138.67, 172.89
E	3.667	36.33, 172.89
F	2.847	44.03, 172.89

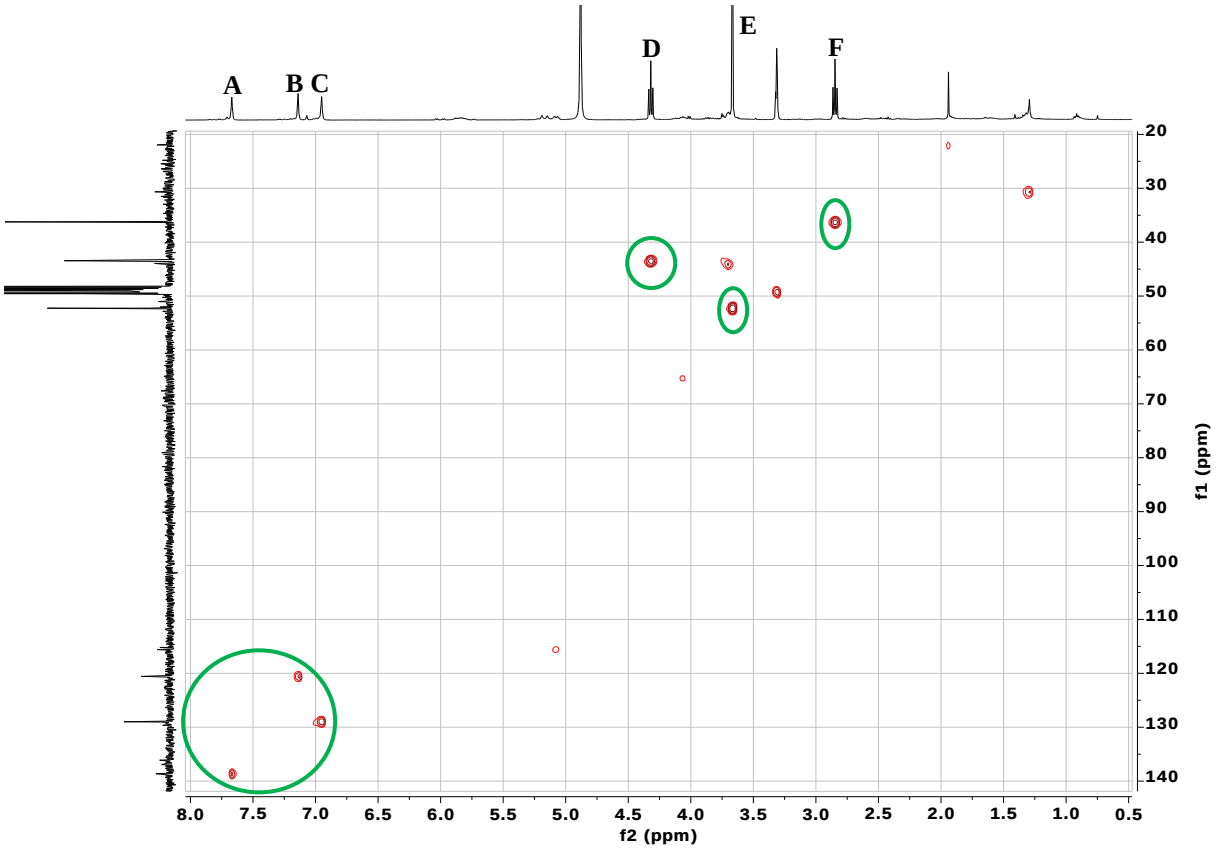

Figure 28. 2D HSQC NMR spectrum of the amide coupling reaction between the tri- & tetra-adduct mixture and allyl amine after column purification, with the ^{1}H NMR spectrum on the x-axis and the ^{13}C NMR spectrum on the y-axis. Circled signals belonging to peaks A-F are analysed below. Obtained in CD_3OD.

Table 7. Peak analysis of the 2D HSQC NMR spectrum

Peak	^{1}H NMR signal (ppm)	^{13}C NMR signals (ppm)
A	7.669	138.67
B	7.139	120.63
C	6.951	129.04
D	4.319	44.03
E	3.667	52.34
F	2.847	36.33

MS spectra

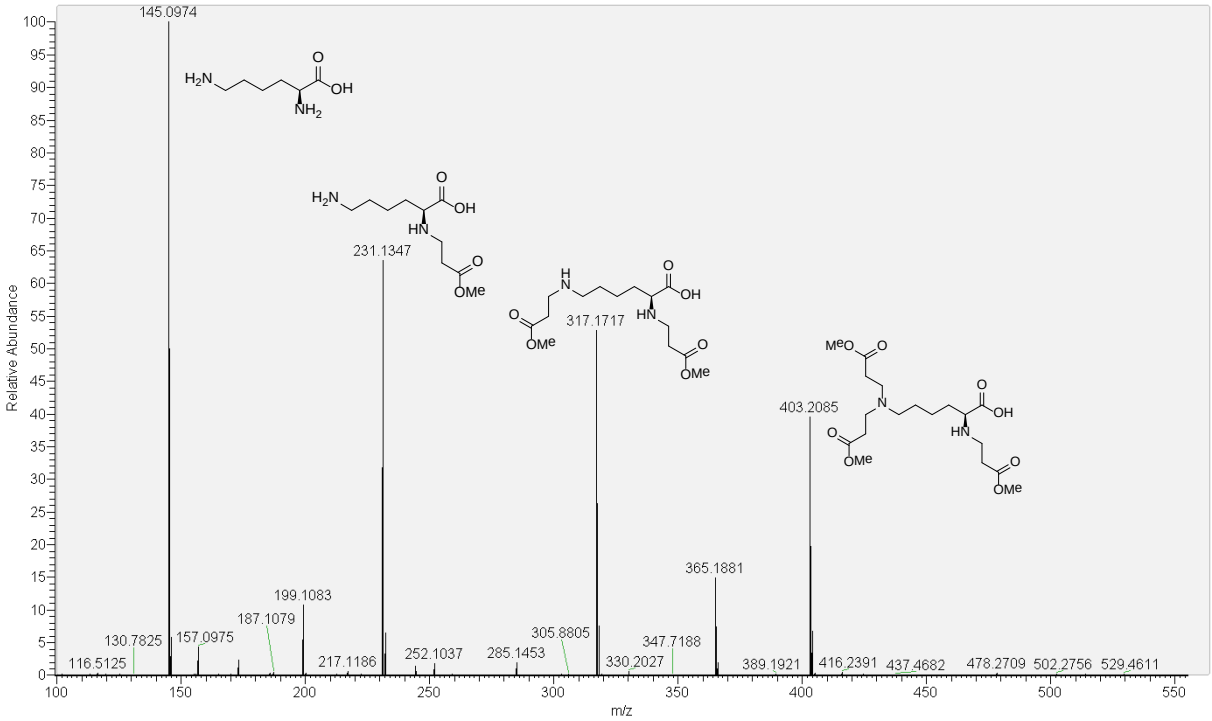

Figure 29. Aza-Michael addition with L-lysine and methyl acrylate at 0 ºC after 20 min. All peaks are [M-H]⁻ adduct ions.

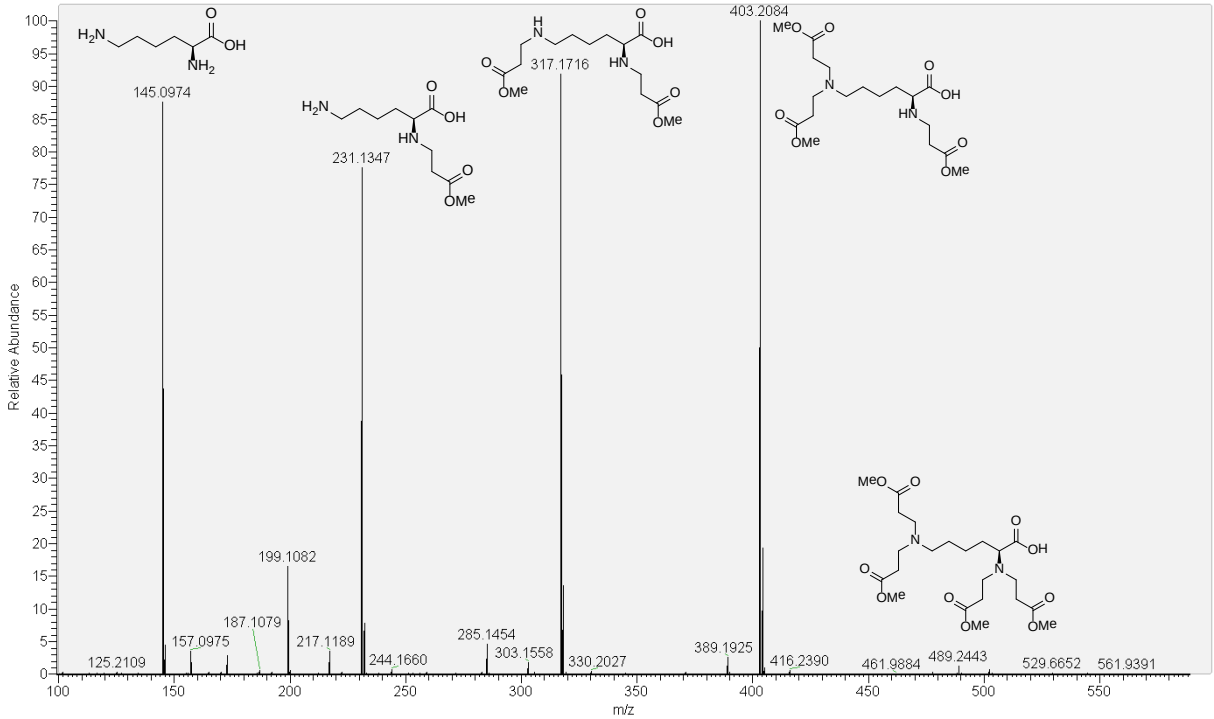

Figure 30. Aza-Michael addition with L-lysine and methyl acrylate at 0 ºC after 40 min. All peaks are [M-H]⁻ adduct ions. The peak for the tetra-adduct is visible at m/z = 489.2443.

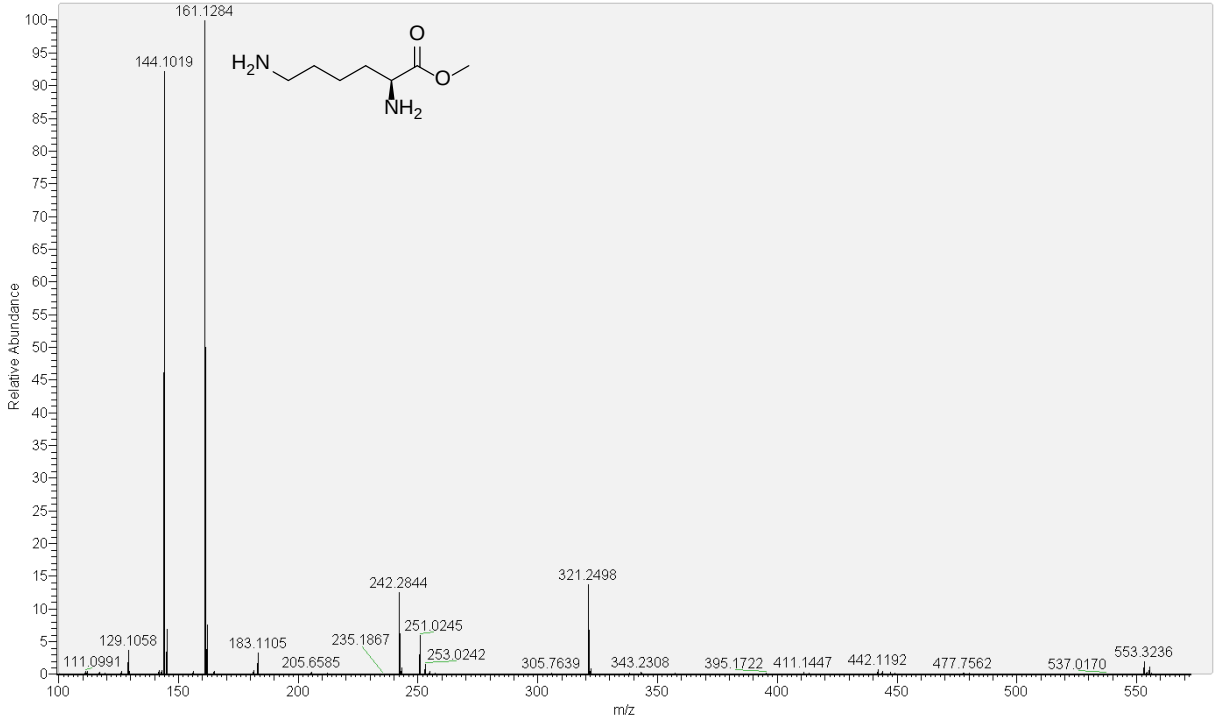

Figure 31. MS spectrum of the aza-Michael addition with L-lysine methyl ester and tert-butyl acrylate at 0 °C after 40 minutes. The peak at m/z = 161.1284 corresponds to the $[M+H]^+$ of L-lysine methyl ester (structure shown).

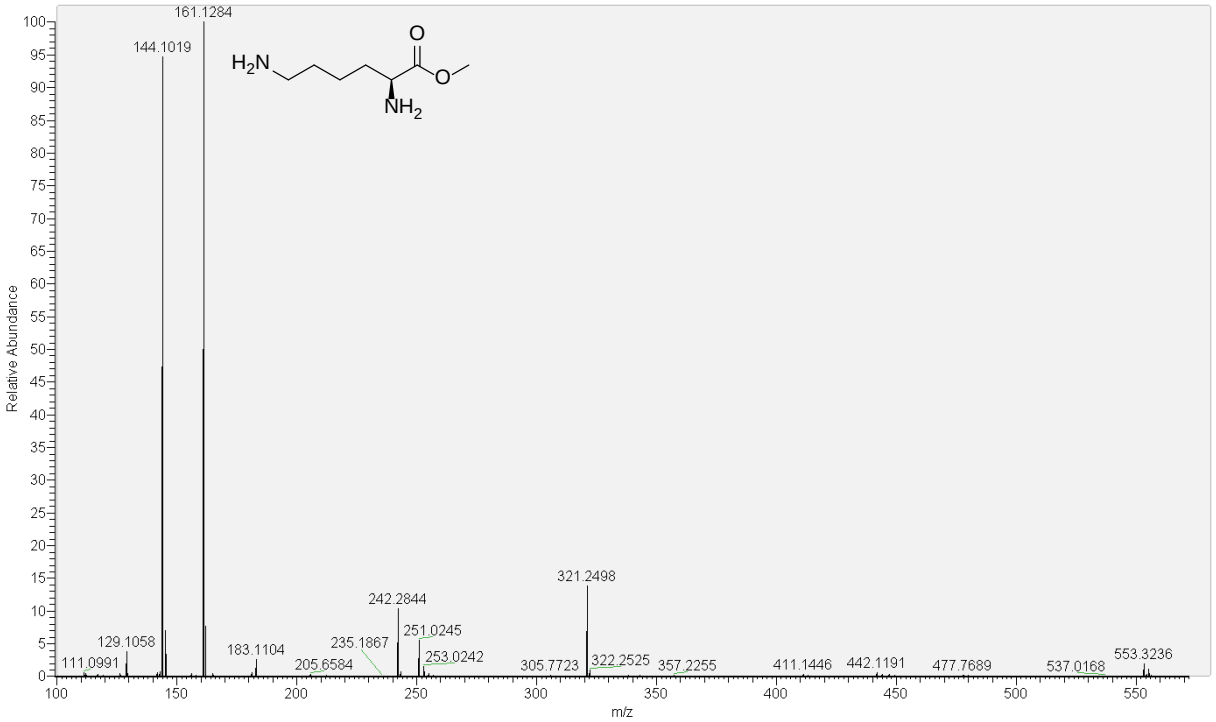

Figure 32. MS spectrum of the aza-Michael addition with L-lysine methyl ester and tert-butyl acrylate at 0 °C after 60 minutes. The peak at m/z = 161.1284 corresponds to the $[M+H]^+$ of L-lysine me thyl ester (structure shown).

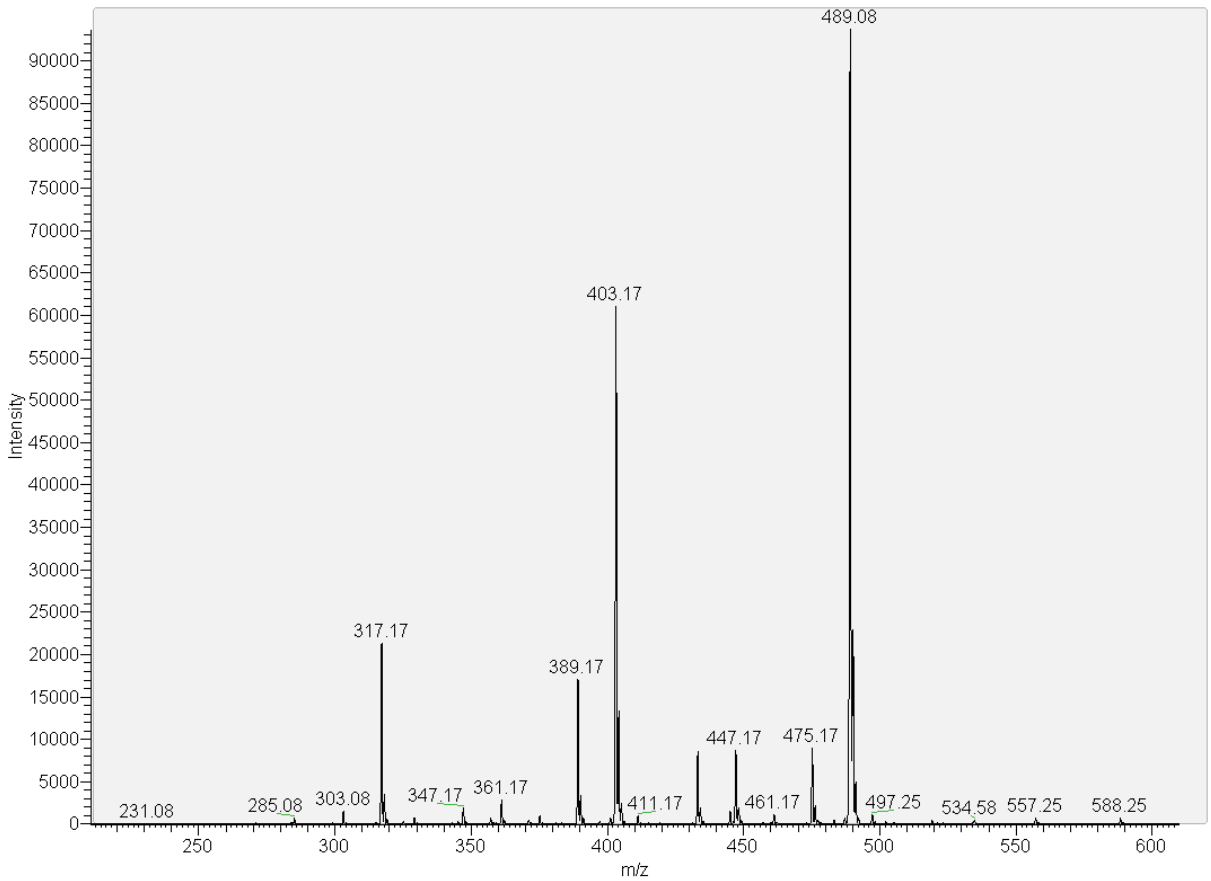

Figure 33. MS spectrum (negative mode) of the aza-Michael addition with L-lysine and methyl acrylate after 48 hours.

Table 8. Peak analysis of the MS spectrum of the aza-Michael addition with L-lysine and methyl acrylate after 48 hours. All peaks are [M-H]$^-$ adduct ions.

m/z	Compound
317.17	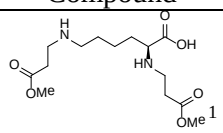 1
389.17	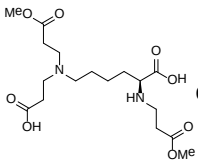 or 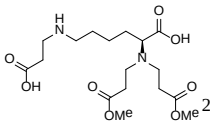 2
403.17	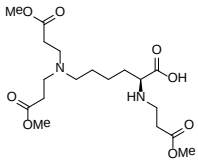 or 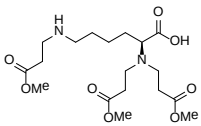
475.17	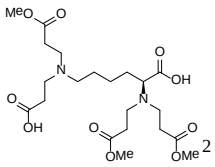 2

489.08		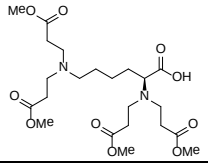

[1]Multiple structures are possible caused by several options for methyl acrylate addition

[2]Multiple structures are possible caused by several options for methyl ester hydrolysis

Table 9. Peak analysis of the MS spectrum of an aza-Michael addition of methyl acrylate and L-lysine, reacted for 11 days

m/z	Adduct ion	Compound
277.25	$[M+2Na-H]^+$	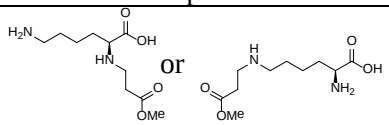 or
319.33	$[M+H]^+$	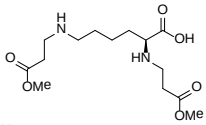
391.33	$[M+H]^+$	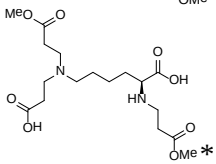 *
405.42	$[M+H]^+$	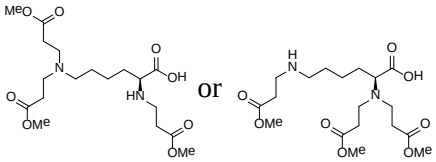 or
491.42 513.42 535.42	$[M+H]^+$ $[M+Na]^+$ $[M+2Na-H]^+$	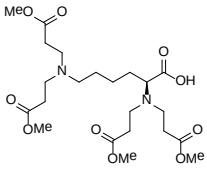
577.50 599.42	$[M+H]^+$ $[M+Na]^+$	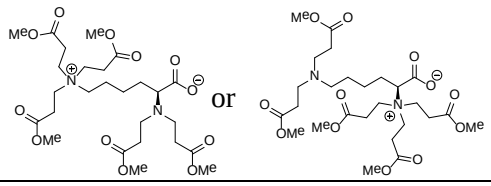 or

* Multiple structures are possible caused by several option for methyl ester hydrolysis